Localization and protein-protein interactions of protein kinase CK2 suggest a chaperone-like activity is integral to its function in *M. oryzae*

Lianhu Zhang[1*], Dongmei Zhang[1*], Yunyun Chen[1], Wenyu Ye[2], Qingyun Lin[2], Guodong Lu[1], Daniel J. Ebbole[1,3], Stefan Olsson[1,4,§] & Zonghua Wang[1,2,5§]

[1]*State Key Laboratory for Ecological Pest Control of Fujian and Taiwan Crops, College of Plant Protection, Fujian Agriculture and Forestry University, Fuzhou 350002, China.*
[2]*College of Life Sciences, Fujian Agriculture and Forestry University, Fuzhou 350002, China.*
[3]*Department of Plant Pathology and Microbiology, Texas A&M University, College Station, Texas 77843, U.S.A.*
[4]*Plant Immunity Center, Haixia Institute of Science and Technology, Fujian Agriculture and Forestry University, Fuzhou 350002, China.*
[5]*Minjing University, Fuzhou 350018, China.*

*These authors contributed equally to this work

§ These authors jointly supervised the work

Abstract

CK2 is known as a constitutively active, conserved serine/threonine kinase in eukaryotes. GFP fusions to CK2 subunits demonstrated nucleolar localization, although the catalytic subunit still localized to nucleoli in the absence of either regulatory subunit. In contrast, localization near septa, required all three subunits. The ~1300 proteins co-immunoprecipitating with the catalytic subunit were highly enriched for those known to reside at these locations. Appressoria contain a filamentous form of CK2. The interacting proteins in hyphae were enriched for intrinsically disordered proteins with characteristics previously identified as being a mechanism for regulation of protein aggregation. Examining gene expression profiles, we find a correlation of CK2 expression with genes for protein disaggregation and

autophagy. Our observations support the view that CK2 plays a key role in controlling formation of discrete regions (membraneless organelles), such as the nucleolus, through aggregation and disaggregation of some of its target proteins.

Introduction

Since its discovery (Meggio and Pinna, 2003), the constitutive serine/threonine (S/T) kinase activity of CK2 and the increasing number of proteins it has been shown to phosphorylate have puzzled scientists (Ahmad et al., 2008; Götz and Montenarh, 2016; Meggio and Pinna, 2003). Indeed CK2 has been implicated in a wide range of cellular processes (Götz and Montenarh, 2016). The CK2 holoenzyme is a heterotetrameric structure consisting of 2 catalytic α-units and 2 regulatory β-subunits (Ahmad et al., 2008). In mammals, there exist two different alpha subunits α (a1) and α' (a2) and the enzyme can contain any combination of α-subunits (α1α1, α1α2, α2α2) combined with the β-subunits. In *Saccharomyces cerevisiae*, CK2 contains two different alpha- and two different β-subunits (b1 and b2) (Padmanabha et al., 1990). CK2 has been extensively studied in the budding yeast *S. cerevisiae* (Padmanabha et al., 1990), however, functions of CK2 involved in multicellularity might be obscured in yeast. For fungi, it has been reported that deletion of both catalytic subunits is lethal (Padmanabha et al., 1990; Wang et al., 2011) and some fungi, including *M. oryzae*, contain only one gene encoding CKa (Mehra et al., 2009). In comparison to yeast, filamentous fungi have different cell types that allow detailed exploration of cellular differentiation and multicellular development (Shlezinger et al., 2012) and this, in combination with haploid life-cycles, well characterized genomes, and efficient methods for targeted gene replacement, makes fungi like *M. oryzae* and *Fusarium graminearum* good model systems for molecular studies of basic eukaryote functions including cell-cell

communication (Cavinder et al., 2012; Ebbole, 2007). As plant pathogens, developmental processes needed for symbiosis can also be explored. We focused our study on *M. oryzae* one of the most important rice crop pathogens worldwide (Dean et al., 2012).

Our results show that *M. oryzae* CK2 holoenzyme (MoCK2) accumulates in the nucleolus, localizes in structures near septal pores, and assembles to form a large ring structure perpendicular to the appressorium penetration pore. The large-scale structures formed by CK2 protein kinase, combined with our finding of the interaction of CK2 with substrates associated with the location of CK2 enzyme aggregation, suggests that CK2 may control substrate stability and localization near their sites of action. Furthermore, CK2 interacts preferentially with proteins annotated as being intrinsically disordered. Taken together, this work provides further evidence supporting the view (Zetina, 2001) that one of the roles for the CK2 holoenzyme is to induce conformational changes in intrinsically disordered proteins.

RESULTS

Deletion of MoCK2 components

Using BLASTp and the protein sequences for the CK2 catalytic subunits of *S. cerevisiae,* CKa1, CKa2, CKb1 and CKb2 (Padmanabha et al., 1990), we identified one MoCKa (MGG_03696) and two MoCKb sequences (MoCKb1 = MGG_00446, MoCKb2 = MGG_05651) (Figure 1). Sequence alignments and phylogenetic analysis show that these proteins are highly conserved in different fungi (Figure 1 Supplement 1-4). Moreover, the phylogenetic analysis indicated that the two CKbs were in two separate evolutionary branches (Figure 1 Supplement 1).

80 We attempted targeted deletions of the three identified genes and succeeded in
81 deleting the two *CKb* genes but not the *CKa* and then also saw that the conidial
82 morphology was different in the CKb mutants in that they had fewer conidial
83 compartments (Figure 2).

84

85 **Subcellular localization of CK2 subunits**

86 To assess the localization of the three CK2 subunits, we constructed N-terminal GFP
87 fusions of all three proteins (Filhol et al., 2003) (GFP-MoCKa, GFP-MoCKb1 and
88 GFP-MoCKb2) (Table 1). All three strains showed the same growth, morphology and
89 pathogenicity (Figure 3) as the background strain Ku80. The CKa and CKb1&2
90 fusion proteins localized to nuclei and prominently to nucleoli and, interestingly, to
91 both sides of septal pores in hyphae (Figure 4 a-e) and conidia (Figure 4 Supplement
92 1). We then tested if the localization to septa and nucleoli were dependent on the
93 association with the other subunits of the holoenzyme. We had measured MoCka
94 expression in the two *MoCkb* mutants using qPCR and noted it was downregulated
95 compared to the background strain Ku80 (Figure 5 a). Thus, we constructed strains
96 that over-express GFP-CKa in the *ΔMockb1* and *ΔMockb2* deletion strains (43OE and
97 53OE respectively, Figure 5 b-e) but this did not result in localization to septa (Figure
98 4 f,g). However, nucleolar localization of GFP-MoCKa was clear even in the
99 *MoCKb1* and *MoCKb2* mutant backgrounds. To test if over-expression of any one of
100 the CKb proteins could rescue the effect of the deletion of the other CKb, we
101 constructed GFP-CKb overexpression strains in the background strain Ku80 and both
102 CKb mutants. These strains were GFP-CKb1 in *ΔMockb2* (54OE-GFP) and GFP-
103 CKb2 in *ΔMockb1* (45OE-GFP). The overexpression of either of the two CKbs in the
104 background strain Ku80 showed normal localization to septa and nucleolus but the
105 overexpression in the deletion strains could not rescue normal localization (Figure

106 4h,i and Figure 5 Supplement 1). Furthermore, GFP-MoCKb1 appeared to localize to
107 nuclei but not nucleoli in the *MoCKb2* mutant. Similarly, GFP-MoCKb2 also
108 appeared to localize to nuclei but not nucleoli in the *MoCKb1* mutant. Conidia
109 morphology also changed in the *ΔMockb2* deletion mutants (Figure 2c), even if CKa
110 was overexpressed as in 43OE and 53OE (Figure 5), which restored some of the
111 conidia formation and growth rate defects (Figure 5). These conidia mainly contained
112 2 nuclei instead of the normal 3 found in the background strain Ku80 (Figure 2c,
113 Figure 5 d,e).

114

115 **Infection phenotypes of CKb deletions**

116 Deletion of CK2 genes has been shown to have effects on both growth and infection
117 in *F. graminearum* (Wang et al., 2011) and we also found this to be the case for *M.*
118 *oryzae* (Figure 6 and Figure 6 Supplement 1). Conidiation was virtually absent in
119 *ΔMockb1* and *ΔMockb2* deletion mutants, thus, we used mycelial plugs to test for
120 infection (Liu et al., 2010; Talbot et al., 1996). Compared to the background strain
121 Ku80, all mutants lacking one of the MoCK2b components had severely reduced or
122 absent pathogenicity even if the other MoCK2 components were over-expressed
123 (Figure 6c).

124

125 **CKa localization in appressoria**

126 Since we found large effects in infection of the deletion of the CKb components we
127 decided to investigate localization of GFP-CKa in the appressoria of the background
128 strain Ku80 and the two CKb deletion mutants. Normal appressoria were only formed
129 in the background strain Ku80 and in these, CK2 localizes to nuclei (Figure 7a top
130 row and Figure 7 Supplement 1b), to the septa between the appressorium and the

germ tube (Figure 7 Supplement 1) and also assembles a large ring structure perpendicular to the penetration pore (Figure 7 b-d, Figure 7 Supplement 1, Figure 7 Supplement 2 for ring size measurements, and movies associated with the images of Figure 7b-d, showing 3D rotations to visualize the ring and the appressorium). MoCKa nuclear localization was present but ring structures were absent in appressoria formed by the two CK2b deletion mutants (Figure 7a middle and bottom row). As can be seen in Figure 7d, the CK2 large ring structure is positioned perpendicular to the penetration pore where the F-actin-septin ring has been shown to form around the pore opening (Dagdas et al., 2012) (Figure 7d and 8 schematic drawing).

Identification of potential septal and nucleolar substrates for MoCK2 by GFP-CKa pulldown

The localization pattern suggested that CK2 may have substrates associated with septa and nucleolar function. To explore this, we performed co-immunoprecipitation to identify proteins interacting with CK2 using GFP-CKa as a "bait", and in addition to the bait, identified 1505 proteins (Supplementary File 1). We also searched the *M. oryzae* proteome for proteins containing the CK2 phosphorylation helix unfolding motif identified by Zetina (Zetina, 2001) using the FIMO tool at the MEMEsuit website (http://meme-suite.org/) and found 1465 proteins (Supplementary File 2) with the motif, out of a total of 12827 proteins annotated for *M. oryzae.*

There is the risk of false positives in the pulldown. We estimated the number of false positives and removed 155 (~10%) of the lower abundance proteins to arrive at a list of 1350 CKa interacting proteins (see Methods). We found 275 of these proteins contain at least one unfolding motif for alpha helixes. Thus, there is an overrepresentation of the motif among the pulldown proteins (Supplementary File 2)

157 (P-value for the null hypothesis of same frequency as in the whole proteome = 4 E-19,
158 Fisher's Exact test) lending support for the proposed role for this motif as a target for
159 CK2 phosphorylation and protein unfolding. As expected, the pulldown caught both
160 CKb proteins.

161 Since CK2 localizes to septa we looked for known septal proteins in the pulldown.
162 All previously identified proteins by Dagas et al. (Dagdas et al., 2012) that are
163 involved in appressorium pore development, were found in the pulldown as was a
164 protein annotated as the main Woronin body protein, Hex1 (MGG_02696). Since the
165 Woronin body in Ascomycetes is tethered to the septal rim by Lah protein (Han et al.,
166 2014; Ng et al., 2009; Plamann, 2009) we searched for a homologue in *M. oryzae* and
167 found a putative MoLah (MGG_01625) with a similar structure as in *Aspergillus*
168 *oryzae* (Han et al., 2014) that is also present in the pulldown. In addition to the Lah,
169 18 other intrinsically disordered septal pore associated proteins (Spa) were described
170 for *Neurospora crassa* (Lai et al., 2012). We identified putative orthologs for 15 of
171 the 18 Spa proteins in *M. oryzae* (Supplementary File 3). Of these putative MoSpa
172 proteins, six were present in the CKa pulldown, Spa3 (MGG_02701), Spa5
173 (MGG_13498), Spa7 (MGG_15285), Spa11 (MGG_16445), Spa14 (MGG_03714)
174 and Spa 15 (MGG_15226). Spa3, Spa5 and Spa15 also contain the CK2
175 phosphorylation alpha helix unfolding motif (Supplementary File 1).

176 To further explore the hypothesis that CK2 could interact with and possibly
177 phosphorylate intrinsically unfolded proteins we used the FuncatDB
178 (http://mips.helmholtz-muenchen.de/funcatDB/) to make a functional classification of
179 the pulldown proteins including those containing the alpha helix unfolding motif
180 (Zetina, 2001). We found strong overrepresentation for proteins involved in rRNA
181 processing among the pulldown proteins containing the alpha helix unfolding motif
182 as well as for proteins that, themselves, are known to interact with other proteins,
183 DNA, and RNA (Supplementary File 4). These classes of proteins are enriched for

184 intrinsically disordered proteins. Such intrinsically disordered proteins can interact
185 with each other to form ordered subregions that have been described as
186 membraneless organelles, such as nucleoli (Wright and Dyson, 2015). Since CK2
187 localizes to the nucleolus we were especially interested in the interaction of CK2 with
188 nucleolar localized proteins. We identified homologues to the well described *S.*
189 *cerevisiae* nucleolar proteins and found a total of 192 proteins in *M. oryzae*
190 homologous to yeast nucleolar proteins (Supplementary File 5). We found 120 (63%)
191 of the nucleolar proteins in the pulldown and 60 of these (50%) had the alpha helix
192 unfolding motif (Supplementary File 1 and 4). The nucleolar proteins were highly
193 overrepresented in the pulldown (P-value for the null hypothesis of same frequency
194 as in the whole proteome 9E-43 Fisher's Exact test) (Supplementary File 5)
195 compared to the whole proteome as was also nucleolar proteins having the unfolding
196 motif (P-value for the null hypothesis of same frequency as in the whole proteome
197 2E-13 Fisher's Exact test) (Supplementary File 5).

198 Interestingly the pulldown proteins without the unfolding motif were strongly
199 enriched (60 of 130 in the whole proteome, P-value for the null hypothesis of same
200 frequency as in the whole proteome 1.0E-29) for proteins that are imported into
201 mitochondria and involved in oxidative phosphorylation ("02.11 electron transport
202 and membrane-associated energy conservation" category from Funcat)
203 (Supplementary File 4).

204 There was no enrichment for specific pathogenicity related proteins (Funcat category
205 32.05 disease, virulence and defence) (Supplementary File 4). This is generally true
206 within the whole Funcat category related to stress and defence (32 CELL RESCUE,
207 DEFENSE AND VIRULENCE) with the exception of proteins involved in the
208 unfolded protein response (32.01.07 unfolded protein response) (e.g. ER quality
209 control), which were overrepresented. This is notable since an involvement of CK2 in
210 protein import into the ER has be established (Wang and Johnsson, 2005). An

211 association of pathogenicity related proteins with CK2 was not expected because of
212 the *in vitro* growth conditions of the experiment.

213 Interestingly, five putative S/T phosphatases (MGG_03154, MGG_10195,
214 MGG_00149, MGG_03838, MGG_06099) were in the pulldown set of proteins
215 (Supplementary File 1). Conceivably these might de-phosphorylate CKa substrates as
216 well as substrates of other kinases to expand the reach of CK2 in regulating the
217 phosphoproteome. To examine the relationship between the expression of CK2 and
218 these phosphatases, we downloaded expression data from a range of experiments
219 with *M. oryzae* and plotted the expression of the five phosphatases found in the
220 pulldown and an S/T phosphatase not found in the pulldown as a function of the CKa
221 expression. We found that two of the S/T phosphatases present in the pulldown were
222 strongly correlated with CKa expression and the others were less strongly correlated
223 (Figure 9).

224

225 **CKa expression correlates with expression of genes associated with**
226 **disaggregation and autophagy**

227 Since CK2 activity has the potential to favour protein-protein binding between
228 intrinsically disordered proteins it consequently also has the potential to enhance
229 protein aggregation. Some of these unfolded proteins may trigger the unfolded
230 protein response involved in disaggregation. Hsp104 is a disaggregase that cooperates
231 with Yjdg1 and SSa1 to refold and reactivate previously denatured and aggregated
232 proteins (Glover and Lindquist, 1998). Alternatively, accumulated aggregates may
233 be degraded through autophagy since these kinds of aggregates are too big for
234 proteasome degradation (Wong and Cuervo, 2010). If this is the case, CK2
235 upregulation should be accompanied by higher autophagy flux or at least there should
236 not be low expression of key autophagy genes when CK2 expression is high (Wong

237 and Cuervo, 2010). Atg8 is a key autophagy protein for which its turnover rate can
238 reflect autophagy flux (Klionsky et al., 2016). To test this hypothesis, we used the
239 expression data we downloaded for plant infection experiments with *M. oryzae* and
240 also for another fungal plant pathogen, *F. graminearum*, that has rich transcriptomic
241 data available (see methods), to examine expression of HSP104, YDJ1, SSA1, and
242 ATG8 relative to CKa.

243 For *M. oryzae*, we found an approximately 60-fold increase in MoHSP104 expression
244 associated with a doubling of MoCka transcript levels. With increasing expression of
245 MoCka the MoHSP104 levels did not increase further. MoSSA1 expression had a
246 similar pattern to MoHSP104 with a 16-fold increase across the initial 2-fold increase
247 in MoCka expression. For MoYDJ1, expression increased with MoCKa expression,
248 but not as dramatically (Fig 10). For *M. oryzae*, we find a log-log linear relationship
249 between the MoCKa expression and MoAtg8 expression (Figure 10).

250 In the case of *F. graminearum*, we also found increased expression of all of the genes
251 with FgCKa expression across a large range of experiments (Figure 10 Supplement
252 1a). Within the experiments a time course experiment was selected to examine
253 expression of these genes during the course of infection. Once again, the relationship
254 could be observed (Figure 10 Supplement 1b), furthermore, FgCK2a expression
255 increased during the course of infection (Figure 10 Supplement 2), supporting the
256 hypothesis that protein disaggregation and autophagy are increasingly needed to
257 remove protein aggregates stimulated to form by increasing levels of CKa and its
258 activity in the cell.

259

260 **Discussion**

261 In contrast to *S. cerevisiae* (Padmanabha et al., 1990) and *F. graminearum* (Wang et
262 al., 2011) but consistent with *N. crassa* (Mehra et al., 2009) we only found one CKa

263 encoding gene in *M. oryzae*. In fungi where two different *CKa* genes are found
264 deletion of both is lethal (Padmanabha et al., 1990; Wang et al., 2011), so it is rather
265 expected that we were not able to obtain a *ΔMocka* mutant.

266 The analysis of the *MoCKb* mutants and the localization of the GFP-labelled MoCK2
267 proteins showed that all identified MoCK2 components are needed for normal
268 function and also normal localization. Localization to septa requires all three subunits,
269 presumably as the holoenzyme. Mutation of either CKb subunit blocks nucleolar
270 localization of the other CKb subunit. Surprisingly, nucleolar localization of CKa was
271 observed in the CKb mutants. This shows that the holoenzyme is not required for
272 CKa localization to the nucleolus. It seems likely that CKb1 and CKb2 must interact
273 with each other in order to interact with CKa, and that CKa is required for movement
274 of CKb subunits into the nucleolus as the holoenzyme.

275 The pattern of localization to septa (Figures 4) observed is remarkably similar to that
276 displayed by the Woronin body tethering protein AoLah from *A. oryzae* (Figure 4b in
277 (Han et al., 2014)). Pulldown experiments demonstrate that CK2 interacts with
278 proteins that function in septum formation and function, including the MoLah
279 ortholog, supporting the view that localization of the GFP-fusion proteins gives a
280 proper representation of CK2 localization. Our results thus demonstrate that the
281 MoCK2-holoenzyme assembles as a large complex near, and is perhaps tethered to,
282 septa, possibly through binding to MoLah. Since septal pores in fungi are gated (Shen
283 K-F. et al., 2014), as are gap junctions and plasmodesmata in animal and plant tissue,
284 respectively (Ariazi et al., 2017; Kragler, 2013; Neijssen et al., 2005), CK2 has a
285 potential to play a general role in this gating.

286

287 The crystal structure suggested that CK2 can form filaments and higher-order
288 interactions between CK2 holoenzyme tetramer units, and based on this it has been

289 predicted that autophosphorylation between the units could occur to down-regulate
290 activity (Litchfield, 2003; Poole et al., 2005). Filament formation has been shown to
291 occur *in vitro* (Glover, 1986; Seetoh et al., 2016; Valero et al., 1995) and *in vivo*
292 (Hübner et al., 2014). Several forms of higher order interactions have been predicted,
293 and it has been demonstrated that at least one of these has reduced kinase activity
294 (Poole et al., 2005; Valero et al., 1995). However, in our localization experiments we
295 cannot distinguish if the large structure is due to co-localization of the CK2 with
296 another protein, such as the MoLah ortholog, or if CK2 is in an aggregated form near
297 septa. Since MoLah has the characteristics of an intrinsically disordered protein (Han
298 et al., 2014), and CK2 interacts with some proteins to promote their disordered state,
299 we favour the view that CK2 interacts with MoLah and other proteins to form a
300 complex near septa.

301 Our pulldown experiment with GFP-CKa further showed that there was a strong
302 overrepresentation of proteins interacting with CKa that contain known
303 phosphorylation motifs for unfolding of alpha-helixes and this is what would be
304 expected for intrinsically disordered proteins (Uversky, 2015; Zetina, 2001). The
305 finding of overrepresentation of this signal in the set of CK2 interacting proteins
306 corroborates the previous suggestion that CK2 is involved in the
307 destabilization/binding of intrinsically disordered proteins (Zetina, 2001) and is
308 consistent with the strong accumulation of both CK2 and intrinsically disordered
309 proteins in the nucleolus (Fig. 4a and b) (Frege and Uversky, 2015) and also at pores
310 between cell compartments (Lai et al., 2012) (Figure 4d). In addition, and further
311 supporting this conclusion, the six septal pore associated proteins (SPA) that we find
312 in the CKa pulldown are homologues for intrinsically disordered proteins that are
313 expected to form temporary gels that are used to reversibly plug septal pores and
314 regulate traffic through septa (Lai et al., 2012). CK2 could actively be involved in the
315 gelling/un-gelling of the regions near septa to create a membraneless organelle

316 controlling the flow through septa. As a counterpart to CK2 in gelling/un-gelling,
317 disaggregase activity involving the MoHSP104 complex, may be critical for control
318 of this. The observation of transcriptional co-regulation between CKa and HSP104
319 supports this notion.

320 Previous studies of subcytosolic localization reveals that this enzyme is also
321 associated with import into organelles. CK2 promotes protein import into
322 endoplasmic reticulum (Wang & Johnsson, 2005) and into mitochondria during
323 mitochondrial biogenesis and maintenance (Rao et al., 2011). CK2 phosphorylation
324 has been shown to activate Tom 22 precursors to assemble a functional mitochondrial
325 import machinery (Rao et al., 2011). Although CK2 has been implicated to be located
326 in mitochondria in earlier studies in other organisms no proteomic study of yeast
327 mitochondria has detected the presence of CK2 (Rao et al., 2011), hence, we do not
328 expect MoCK2 to be present in mitochondria. Of special interest was the strong
329 overrepresentation of mitochondrial proteins among the CKa pulldown proteins
330 without the alpha helix phosphorylation unfolding motif (Supplementary File 4).
331 Since these proteins need to be imported into mitochondria in an unfolded state, this
332 may point to the existence of other CKa phosphorylation and unfolding motifs that
333 help keep these proteins unfolded until they reach their destination inside the
334 mitochondria.

335 To have such dynamic function as an unfolder of proteins by phosphorylation, CK2
336 should be partnered with phosphatases as counterparts and their activity may track
337 CK2 activity. Consistent with this possibility, we found that two of the five S/T
338 phosphatases that are present in the pulldown are strongly co-regulated with CKa
339 (Figure 9), further supporting the view that CKa-dependent
340 phosphorylation/dephosphorylation plays a major role in shaping protein interactions.
341 Together with the high expression of CK2 in cells, this suggests an important

342 function of CK2 as a general temporary unfolder of intrinsically disordered proteins
343 that comprise roughly 30 % of eukaryotic proteins (Vucetic et al., 2003).

344 As MoCK2 is present in the cytoplasm and nucleoplasm it could generally assist
345 intrinsically disordered proteins forming larger protein complexes (Uversky, 2015). It
346 also seems to be essential for assembling ribosomes containing large numbers of
347 intrinsically disordered proteins (Uversky, 2015). All these functions also explains
348 why CK2 is needed constitutively (Meggio and Pinna, 2003).

349 In the absence of well-functioning autophagy removing incorrectly formed larger
350 protein aggregates, like those formed in brain cells of Alzheimer's patients (Zare-
351 shahabadi et al., 2015), CK2 activity facilitates protein aggregate formation and
352 hastens the progression of Alzheimer's disease (Rosenberger et al., 2016). Using
353 publicly available transcriptome datasets we could show that CKa expression in *M.*
354 *oryzae* and *F. graminearum* is strongly correlated to disaggregase and Atg8
355 expression (Figure 10), and thus autophagy, giving further support for a relationship
356 of CK2 in facilitating the formation of protein aggregates from intrinsically unfolded
357 proteins that are then subjected to autophagy. As autophagy is important to
358 appressorium development (Liu and Lin, 2008; Kershaw and Talbot, 2009), it will be
359 of interest to further examine the role of the CK2 ring structure during appressorial
360 development and infection. The large ring may be a true filament of CK2 in a
361 relatively inactive state that is a store for CK2 so that upon infection, it can facilitate
362 rapid ribosome biogenesis, appressorial pore function, and other pathogenesis-
363 specific functions.

364 **Conclusion**

365 We conclude that CK2 most likely has an important role in the correct
366 assembly/disassembly of intrinsically disordered proteins as well as allowing these
367 proteins to pass through narrow pores between cell compartments in addition to its

368 already suggested role in organelle biogenesis (Rao et al., 2011). Our results further
369 point to one of the main functions of the CK2 holoenzyme as a general facilitator of
370 protein-protein interactions important for a large range of cellular processes including
371 a potential role for gel formation that creates membraneless organelles at septa
372 through its likely interaction with, and modification of, intrinsically disordered
373 proteins. Most of our evidence for these functions of CK2 is, however, indirect, and
374 future experiments will be needed to directly demonstrate the suggested role for CK2
375 in relation to intrinsically disordered proteins, including the function of septa and
376 appressoria in fungi.

377

378 **Methods**

379 **Fungal strains, culture, and transformation**

380 The *M. oryzae* Ku80 mutant (kindly provided by Professor Jin-Rong Xu Department
381 of Botany and Plant Pathology Purdue University, U.S.A.) of the wild type Guy11
382 strain was used as background strain since it lacks non-homologous end joining
383 which facilitates gene targeting (Villalba et al., 2008). Ku80 and its derivative strains
384 (Table 1) were all stored on dry sterile filter paper and cultured on complete medium
385 (CM: 0.6% yeast extract, 0.6% casein hydrolysate, 1% sucrose, 1.5% agar) or starch
386 yeast medium (SYM: 0.2% yeast extract, 1% starch, 0.3% sucrose, 1.5% agar) at
387 25ºC. For conidia production, cultures were grown on rice bran medium (1.5% rice
388 bran, 1.5% agar) with constant light at 25ºC. Needed genome and proteome FASTA
389 files was downloaded from an FTP-server at the Broad Institute
390 (ftp://ftp.broadinstitute.org/pub/annotation/fungi/magnaporthe/genomes/magnaporthe
391 _oryzae_70-15_8/). Fungal transformants were selected for the appropriate markers
392 inserted by the plasmid vectors. The selective medium contained either 600 µg/ml of
393 hygromycin B or 600 µg/ml of G418 or 50 µg/ml chlorimuron ethyl.

394

395 **MoCKb gene replacement and complementation**

396 Gene replacement mutants of *MoCKb1* encoding protein MoCKb1 were generated by
397 homologous recombination. Briefly, a fragment about 0.9 Kb just upstream of
398 *Mockb1* ORF was amplified with the primers 446AF and 446AR (Table 2), so was
399 the 0.7Kb fragment just downstream of *Mockb1* ORF amplified with the primers
400 446BF and 446BR (Table 2). Both fragments were linked with the hygromycin
401 phosphotransferase (*hph*) gene amplified from pCX62 (containing the fragment of
402 TrpC promoter and hygromycin phosphotransferase (*hph*) gene, HPH resistance).
403 Then the fusion fragments were transformed into protoplasts of the background strain
404 Ku80. The positive transformant *ΔMockb1* was picked from a selective agar medium
405 supplemented with 600 μg/ml of hygromycin B and verified by Southern blot.

406 For complementation of the mutant, fragments of the native promoter and gene
407 coding region were amplified using the primers 446comF and 446comR listed Table
408 2. This fragment was inserted into the pCB1532 to construct the complementation
409 vector using the XbaI and KpnI. Then this vector was transformed into the
410 protoplasts of the *ΔMockb1* mutant. The positive complementation transformant
411 MoCKb1C was picked up from the selective agar medium supplemented with
412 50μg/ml chlorimuron ethyl.

413 As for the *ΔMoCKb1* deletion mutant, we constructed a knockout vector to delete the
414 *MoCKb2* from the background strain Ku80. All the primers are listed in the Table 2.
415 The 1.0Kb fragment upstream of *MoCKb2* ORF was amplified with the primers
416 5651AF and 5651AR, inserted into the plasmid pCX62 using the KpnI and EcoRI to
417 get the pCX-5A vector. The 1.0Kb fragment downstream of *Mockb2* ORF was
418 amplified with the primers 5651BR and 5651BR, inserted into the vector pCX-5A
419 using BamHI and XbaI to construct the knockout vector pCX-5D. Then this vector

420 was transformed into the protoplasts of Ku80. The positive transformants were
421 picked up from the selective medium supplemented with the 600 μg/ml hygromycin
422 B. For complementation of the mutant, fragments of the native promoter and gene
423 coding region were amplified using the primers 5651comF and 5651comR listed in
424 the Table 2. This fragment was inserted into pCB1532 to construct the
425 complementation vector using the XbaI and XmaI. Then this vector was transformed
426 into protoplasts of the *ΔMockb2* mutant. The positive complementation transformant
427 MoCKb2C was picked up from the selective agar medium supplemented with 50
428 μg/ml chlorimuron ethyl.

429 **The construction of localization vectors**

430 In order to detect the localization of MoCK2, we constructed localization vectors.
431 The vector pCB-3696OE containing the RP27 strong promoter was used to detect the
432 localization of GFP-MoCKa. The vector pCB-446OE expressed under RP27 strong
433 promoter was used to detect the localization of GFP-MoCKb1. The vector pCB-
434 5651OE expressed by RP27 strong promoter was used to detect the localization of
435 GFP-MoCKb2.

436 **Analysis of conidial morphology, conidial germination and appressoria formation**

437 Conidia were prepared from cultures grown on 4% rice bran medium. Rice bran
438 medium was prepared by boiling 40g rice bran (can be bought for example through
439 Alibaba.com) in 1L DD-water for 30 minutes. After cooling pH was adjusted from to
440 6.5 using NaOH and 20 g agar (MDL No MFCD00081288) was added before
441 sterilization by autoclaving (121 ^{o}C for 20 minutes). Conidia morphology was
442 observed using confocal microscopy (Nikon A1^{+}). The Conidial germination and
443 appressoria formation were incubated on hydrophobic microscope cover glass
444 (Beckerman and Ebbole, 1996) (Fisherbrand) under 25℃ in the dark. Conidial

445 germination and appressoria formation were examined at 24 h post-incubation
446 (Beckerman and Ebbole, 1996; Ding et al., 2010).

447 **Pathogenicity assay**

448 Plant infection assays were performed on rice leaves. The rice cultivar used for
449 infection assays was CO39. In short, mycelial plugs were put on detached intact
450 leaves or leaves wounded by a syringe stabbing. These leaves were incubated in the
451 dark for 24h and transferred into constant light and incubated for 5 days to assess
452 pathogenicity (Talbot et al., 1996). For infections using conidial suspensions (1×10^5
453 conidia/ml in sterile water with 0.02% Tween 20) were sprayed on the rice leaves of
454 2-week-old seedlings.

455 **RNA extraction and real-time PCR analysis**

456 RNA was extracted with the RNAiso Plus kit (TaKaRa). First strand cDNA was
457 synthesized with the PrimeScript RT reagent Kit with gDNA Eraser (TaKaRa). For
458 quantitative real-time PCR, *MoCKa, MoCKb1*, and *MoCKb2* were amplified with the
459 primers listed in Table 2. β-tubulin (XP_368640) was amplified as an endogenous
460 control. Real-time PCR was performed with the TaKaRa SYBR Premix Ex Taq
461 (Perfect Real Time) (Takara). The relative expression levels were calculated using
462 the $2^{-\Delta\Delta Ct}$ method (Livak and Schmittgen, 2001).

463 **Pulldown and identification of CKa interacting proteins**

464 Total protein samples were extracted from vegetative mycelia of strain GFP-MoCKa
465 and incubated with anti-GFP beads (Chromotek, Hauppauge, NY, USA) 90 minutes
466 at 4°C with gentle shaking. After a series of washing steps, proteins bound to anti-
467 GFP beads were eluted following the manufacturer's instruction. The eluted proteins
468 were sent to BGI Tech (Shenzhen, Guangdong province, China) and analysed by
469 mass spectrometry for analysis of sequence hits against the *M. oryzae* proteome. The

470 transformant expressing GFP protein only was used as the negative control and the
471 Ku80 was used as Blank control. Data from three biological replicates were analyzed
472 against the background of proteins that were bound non-specifically to the anti-GFP
473 beads in GFP transformant and in WT to get the final gene list of genes that was
474 pulldown with CKa (Supplementary File1).

475 **Estimation of non-specific binding of proteins in the pulldown**

476 We developed two methods to estimate the number of non-specific binding proteins
477 found in the CKa pulldown. The first approach is a chemistry-based reasoning and
478 assumes that the degree of unspecific association to the protein per protein surface
479 area is the same for GFP specific hits and for the CK2 holoenzyme pulled down.
480 Using this technique, we estimate that 44-132 proteins are false positive in the CKa
481 pulldown (all proteins pulled down by GFP-Beads or the Beads already removed
482 from the list) (Supplementary File 1). The Second approach is statistical where we
483 assume that binding of the true interacting proteins to CKa are log-normally
484 distributed related to the abundance of each protein in the pulldown, since the median
485 is low and close to zero and negative amounts are impossible. Using the deviation
486 from the theoretical distribution, with higher than expected amounts of a specific
487 protein, for the less abundant proteins we estimate that 46-81 proteins found in the
488 CKa pulldown (with controls subtracted) were false positive. The higher number was
489 used to set a conservative threshold for which proteins should be included in the
490 analysis (See Supplementary File 1 for details of both methods).

491 **Finding *M. oryzae* proteins containing the helix unfolding motif**

492 The MEME motif LSDDDXE/SLEEEXD (Zetina, 2001) was used to search through
493 the proteome of *M. oryzae* using the FIMO tool at the MEMEsuite website
494 (http://meme-suite.org/). Results were then downloaded and handled in MS Excel to
495 produce a list of proteins with at least one motif hit (Supplementary File 2)

496 **Analysis of CKa expression in relation to disaggregase related protein, Atg8 and**
497 **Ser/Thr phosphatase expression**

498 For *M. oryzae,* transcriptome experiment data was downloaded as sra/fastq files from
499 Gene Expression Omnibus, https://www.ncbi.nlm.nih.gov/geo/and mapped onto the
500 genome found at http://fungi.ensembl.org/Magnaporthe_oryzae/Info/Index. The
501 procedure was the following: Gene Expression Omnibus (Barrett et al., 2012) was
502 queried for SRA files originating from *M. oryzae* and the files downloaded. The
503 conversion from SRA to Fastq was done using the SRA toolkit
504 (http://ncbi.github.io/sra-tools). The resulting samples were subjected to quality
505 control using FASTQC (Andrews, 2010). Quantification of RNA was performed
506 using Kallisto with default settings (Bray 2016), the data was then normalized using
507 the VST algorithm implemented in DESeq2 (Love et al., 2014).

508 For *F. graminearum* transcriptomic data (FusariumPLEX) was directly downloaded
509 for mainly *in planta* experiments from the PlexDB database
510 (http://www.plexdb.org/modules/PD_general/download.php?species=Fusarium). For
511 each fungus an expression matrix with the different experiments as columns and gene
512 id using the FGSG codes according to BROAD
513 (ftp.broadinstitute.org/distribution/annotation/fungi/fusarium/genomes/fusarium_gra
514 minearum_ph-1) as rows were prepared. From the resulting matrixes (Supplementary
515 Files 6 and 7) we used the data needed to plot expression of Atg8 vs CKa for the two
516 fungi. In *M. oryzae* data are expressed as log2 of RPKM values. Similarly, for *F.*
517 *graminearum*, data were log2 of reported relative expression. Gene expression data
518 used were from MoCKa, MoHSP104, FgHSP109, MoYDJ1, FgYDJ1, MoSSA1and
519 Fg SSA1 homologues identified in this study as well as from MoAtg8 (MGG_01062)
520 (Veneault-Fourrey, 2006), FgCKa (FGSG_00677) (Wang et al., 2011) and FgAtg8
521 (FGSG_10740) (Josefsen et al., 2012). Data from the *M. oryzae* expression matrix

522 was also used for plotting MoCKa expression versus the expression of annotated
523 serine/threonine phosphatases found in the CKa pulldown.

524 **Data availability**

525 The data that support the findings of this study are available from the corresponding
526 authors upon reasonable request.

527

528 **References**

529 Ahmad, K.A., Wang, G., Unger, G., Slaton, J., and Ahmed, K. (2008). Protein kinase CK2 – A key
530 suppressor of apoptosis. Adv. Enzyme Regul. *48*, 179–187.

531 Andrews, S. (2010). FastQC: a quality control tool for high throughput sequence data. Available
532 online at http://www.bioinformatics.babraham.ac.uk/projects/fastqc.

533 Ariazi, J., Benowitz, A., De Biasi, V., Den Boer, M.L., Cherqui, S., Cui, H., Douillet, N., Eugenin,
534 E.A., Favre, D., Goodman, S., et al. (2017). Tunneling Nanotubes and Gap Junctions–Their Role in
535 Long-Range Intercellular Communication during Development, Health, and Disease Conditions.
536 Front. Mol. Neurosci. *10*.

537 Barrett, T., Wilhite, S.E., Ledoux, P., Evangelista, C., Kim, I.F., Tomashevsky, M., Marshall, K.A.,
538 Phillippy, K.H., Sherman, P.M., Holko, M., et al. (2012). NCBI GEO: archive for functional
539 genomics data sets—update. Nucleic Acids Res. *41*, D991–D995.

540 Beckerman, J.L., and Ebbole, D.J. (1996). MPG1, a Gene Encoding a Fungal Hydrophobin of
541 Magnaporthe grisea, Is Involved in Surface Recognition. MPMI *9*, 450–456.

542 Cavinder, B., Sikhakolli, U., Fellows, K.M., and Trail, F. (2012). Sexual Development and
543 Ascospore Discharge in Fusarium graminearum. J. Vis. Exp.

544 Dagdas, Y.F., Yoshino, K., Dagdas, G., Ryder, L.S., Bielska, E., Steinberg, G., and Talbot, N.J.
545 (2012). Septin-mediated plant cell invasion by the rice blast fungus, Magnaporthe oryzae. Science
546 *336*, 1590–1594.

547 Dean, R., Van Kan, J.A.L., Pretorius, Z.A., Hammond-Kosack, K.E., Di Pietro, A., Spanu, P.D.,
548 Rudd, J.J., Dickman, M., Kahmann, R., Ellis, J., et al. (2012). The Top 10 fungal pathogens in
549 molecular plant pathology: Top 10 fungal pathogens. Mol. Plant Pathol. *13*, 414–430.

550 Ding, S.-L., Liu, W., Iliuk, A., Ribot, C., Vallet, J., Tao, A., Wang, Y., Lebrun, M.-H., and Xu, J.-R.
551 (2010). The Tig1 Histone Deacetylase Complex Regulates Infectious Growth in the Rice Blast
552 Fungus Magnaporthe oryzae. PLANT CELL ONLINE *22*, 2495–2508.

553 Ebbole, D.J. (2007). Magnaporthe as a Model for Understanding Host-Pathogen Interactions. Annu.
554 Rev. Phytopathol. *45*, 437–456.

555 Filhol, O., Nueda, A., Martel, V., Gerber-Scokaert, D., Benitez, M.J., Souchier, C., Saoudi, Y., and
556 Cochet, C. (2003). Live-Cell Fluorescence Imaging Reveals the Dynamics of Protein Kinase CK2
557 Individual Subunits. Mol. Cell. Biol. *23*, 975–987.

558 Frege, T., and Uversky, V.N. (2015). Intrinsically disordered proteins in the nucleus of human cells.
559 Biochem. Biophys. Rep. *1*, 33–51.

560 Glover, C.V. (1986). A Filamentous Form of Drosophila Casein Kinase II. J. Biol. Chem. *261*,
561 14349–14354.

562 Glover, J.R., and Lindquist, S. (1998). Hsp104, Hsp70, and Hsp40: A Novel Chaperone System that
563 Rescues Previously Aggregated Proteins. Cell *94*, 73–82.

564 Götz, C., and Montenarh, M. (2016). Protein kinase CK2 in development and differentiation
565 (Review). Biomed. Rep.

566 Han, P., Jin, F.J., Maruyama, J., and Kitamoto, K. (2014). A Large Nonconserved Region of the
567 Tethering Protein Leashin Is Involved in Regulating the Position, Movement, and Function of
568 Woronin Bodies in Aspergillus oryzae. Eukaryot. Cell *13*, 866–877.

569 Hübner, G.M., Larsen, J.N., Guerra, B., Niefind, K., Vrecl, M., and Issinger, O.-G. (2014).
570 Evidence for aggregation of protein kinase CK2 in the cell: a novel strategy for studying CK2
571 holoenzyme interaction by BRET2. Mol. Cell. Biochem. *397*, 285–293.

572 Josefsen, L., Droce, A., Sondergaard, T.E., Sørensen, J.L., Bormann, J., Schäfer, W., Giese, H., and
573 Olsson, S. (2012). Autophagy provides nutrients for nonassimilating fungal structures and is
574 necessary for plant colonization but not for infection in the necrotrophic plant pathogen Fusarium
575 graminearum. *8*, 13.

576 Kershaw, M.J., and Talbot, N.J. (2009). Genome-wide functional analysis reveals that infection-
577 associated fungal autophagy is necessary for rice blast disease. Proc. Natl. Acad. Sci. *106*, 15967–
578 15972.

579 Klionsky, D.J., Abdelmohsen, K., Abe, A., Abedin, M.J., Abeliovich, H., Acevedo Arozena, A.,
580 Adachi, H., Adams, C.M., Adams, P.D., Adeli, K., et al. (2016). Guidelines for the use and
581 interpretation of assays for monitoring autophagy (3rd edition). Autophagy *12*, 1–222.

582 Kragler, F. (2013). Plasmodesmata: intercellular tunnels facilitating transport of macromolecules in
583 plants. Cell Tissue Res. *352*, 49–58.

584 Lai, J., Koh, C.H., Tjota, M., Pieuchot, L., Raman, V., Chandrababu, K.B., Yang, D., Wong, L., and
585 Jedd, G. (2012). Intrinsically disordered proteins aggregate at fungal cell-to-cell channels and
586 regulate intercellular connectivity. Proc. Natl. Acad. Sci. *109*, 15781–15786.

587 Litchfield, D.W. (2003). Protein kinase CK2: structure, regulation and role in cellular decisions of
588 life and death. Biochem. J. *369*, 1–15.

589 Liu, X., and Lin, F. (2008). Investigation of the biological roles of autophagy in appressorium
590 morphogenesis in Magnaporthe oryzae. J. Zhejiang Univ. Sci. B *9*, 793–796.

591 Liu, W., Xie, S., Zhao, X., Chen, X., Zheng, W., Lu, G., Xu, J.-R., and Wang, Z. (2010). A
592 homeobox gene is essential for conidiogenesis of the rice blast fungus Magnaporthe oryzae. Mol.
593 Plant. Microbe Interact. *23*, 366–375.

594 Livak, K.J., and Schmittgen, T.D. (2001). Analysis of Relative Gene Expression Data Using Real-
595 Time Quantitative PCR and the 2−ΔΔCT Method. Methods *25*, 402–408.

596 Love, M.I., Huber, W., and Anders, S. (2014). Moderated estimation of fold change and dispersion
597 for RNA-seq data with DESeq2. Genome Biol. *15*.

598 Meggio, F., and Pinna, L.A. (2003). One thousand-and one substrates of protein kinase CK2.
599 FASEB J. *17*, 349–368.

600 Mehra, A., Shi, M., Baker, C.L., Colot, H.V., Loros, J.J., and Dunlap, J.C. (2009). A Role for
601 Casein Kinase 2 in the Mechanism Underlying Circadian Temperature Compensation. Cell *137*,
602 749–760.

603 Neijssen, J., Herberts, C., Drijfhout, J.W., Reits, E., Janssen, L., and Neefjes, J. (2005). Cross-
604 presentation by intercellular peptide transfer through gap junctions. Nature *434*, 83–88.

605 Ng, S.K., Liu, F., Lai, J., Low, W., and Jedd, G. (2009). A Tether for Woronin Body Inheritance Is
606 Associated with Evolutionary Variation in Organelle Positioning. PLoS Genet. *5*, e1000521.

607 Padmanabha, R., Chen-Wu, J.L.-P., Arnot, D.E., and Glover, C.V.C. (1990). Isolation, sequencing,
608 and disruption of the yeast CKA2 gene casein kinase II is essential for viability in Saccharomyces
609 cerevisiae. Mol. Cell. Biol. *10*, 4089–4099.

610 Plamann, M. (2009). Cytoplasmic Streaming in Neurospora: Disperse the Plug To Increase the
611 Flow? PLoS Genet. *5*, e1000526.

612 Poole, A., Poore, T., Bandhakavi, S., McCann, R.O., Hanna, D.E., and Glover, C.V. (2005). A
613 global view of CK2 function and regulation. Mol. Cell. Biochem. *274*, 163–170.

614 Rao, S., Gerbeth, C., Harbauer, A., Mikropoulou, D., Meisinger, C., and Schmidt, O. (2011).
615 Signaling at the gate: Phosphorylation of the mitochondrial protein import machinery. Cell Cycle
616 *10*, 2083–2090.

617 Rosenberger, A.F.N., Morrema, T.H.J., Gerritsen, W.H., van Haastert, E.S., Snkhchyan, H.,
618 Hilhorst, R., Rozemuller, A.J.M., Scheltens, P., van der Vies, S.M., and Hoozemans, J.J.M. (2016).
619 Increased occurrence of protein kinase CK2 in astrocytes in Alzheimer's disease pathology. J.
620 Neuroinflammation *13*.

621 Seetoh, W.-G., Chan, D.S.-H., Matak-Vinković, D., and Abell, C. (2016). Mass Spectrometry
622 Reveals Protein Kinase CK2 High-Order Oligomerization *via* the Circular and Linear Assembly.
623 ACS Chem. Biol. *11*, 1511–1517.

624 Shen K-F., Osmani A. S., Govindaraghavan M., and Osmani S. A. (2014). Mitotic rregulation of
625 fungal cell-to-cell connectivity through septal pores involves the NIMA kinase. Mol. Biol. Cell *25*,
626 763–775.

627 Shlezinger, N., Goldfinger, N., and Sharon, A. (2012). Apoptotic-like programed cell death in fungi:
628 the benefits in filamentous species. Front. Oncol. *2*.

629 Talbot, N.J., Kershaw, M.J., Wakley, G.E., De Vries, O.M., Wessels, J.G., and Hamer, J.E. (1996).
630 MPG1 encodes a fungal hydrophobin involved in surface interactions during infection-related
631 development of Magnaporthe grisea. Plant Cell Online *8*, 985–999.

632 Uversky, V.N. (2015). The multifaceted roles of intrinsic disorder in protein complexes. FEBS Lett.
633 *589*, 2498–2506.

634 Valero, E., De Bonis, S., Filhol, O., Wade, R.H., Langowski, J., Chambaz, E.M., and Cochet, C.
635 (1995). Quaternary Structure of Casein Kinase 2 - Characterization of Multiple Oligomeric States
636 and Relation with its Catalytic Activity. J. Biol. Chem. *270*, 8345–8352.

637 Veneault-Fourrey, C. (2006). Autophagic Fungal Cell Death Is Necessary for Infection by the Rice
638 Blast Fungus. Science *312*, 580–583.

639 Villalba, F., Collemare, J., Landraud, P., Lambou, K., Brozek, V., Cirer, B., Morin, D., Bruel, C.,
640 Beffa, R., and Lebrun, M.-H. (2008). Improved gene targeting in Magnaporthe grisea by
641 inactivation of MgKU80 required for non-homologous end joining. Fungal Genet. Biol. *45*, 68–75.

642 Vucetic, S., Brown, C.J., Dunker, A.K., and Obradovic, Z. (2003). Flavors of protein disorder.
643 Proteins Struct. Funct. Bioinforma. *52*, 573–584.

644 Wang, X., and Johnsson, N. (2005). Protein kinase CK2 phosphorylates Sec63p to stimulate the
645 assembly of the endoplasmic reticulum protein translocation apparatus. J. Cell Sci. *118*, 723–732.

646 Wang, C., Zhang, S., Hou, R., Zhao, Z., Zheng, Q., Xu, Q., Zheng, D., Wang, G., Liu, H., Gao, X.,
647 et al. (2011). Functional Analysis of the Kinome of the Wheat Scab Fungus Fusarium graminearum.
648 PLoS Pathog. *7*, e1002460.

649 Wong, E., and Cuervo, A.M. (2010). Integration of Clearance Mechanisms: The Proteasome and
650 Autophagy. Cold Spring Harb. Perspect. Biol. *2*, a006734–a006734.

651 Wright, P.E., and Dyson, H.J. (2015). Intrinsically disordered proteins in cellular signalling and
652 regulation. Nat. Rev. Mol. Cell Biol. *16*, 18–29.

653 Zare-shahabadi, A., Masliah, E., Johnson, G.V.W., and Rezaei, N. (2015). Autophagy in
654 Alzheimer's disease. Rev. Neurosci. *26*.

655 Zetina, C.R. (2001). A Conserved Helix-Unfolding Motif in the Naturally Unfolded Proteins.
656 Proteins Struct. Funct. Genet. *44*, 479–483.

657

Acknowledgements We thank Dr. Guanghui Wang, Dr. Wenhui Zheng, Dr. Ya Li and Dr. Huawei Zheng (Fujian Agriculture and Forestry University, Fuzhou, China) for their helpful discussions. We thank Professor Jin-Rong Xu, Department of Botany and Plant Pathology Purdue University, U.S.A. for providing the Ku80 strain. We thank Dr. Bjoern Oest Hansen, Goettingen for help with mapping and constructing the used *M. oryzae* transcriptome datafile from downloaded data. This work was supported by the National Natural Science Foundation of China (U1305211), National Key Research and Development Program of China (2016YFD0300700) and National Natural Science Foundation for Young Scientists of China (Grant No.31500118 and No.31301630), the 100 Talent Program of Fujian Province, and USDA NIFA Hatch project 1013944.

Authors' contributions Conceived and designed the experiments: G. L., S. O. and Z. W. Performed the experiments: L. Z., D. Z., Y. C., W. Y. and Q. L. Analysed the data: L. Z., D. Z., D. J. E., S. O. and Z. W. Wrote the paper: L. Z., D. Z., D. J. E., S. O. and Z. W.

Competing interests statement The authors declare that they have no competing financial interests.

Correspondence and request for materials should be addressed to S.O. (stefan@olssonstefan.com) or Z.W. (wangzh@fafu.edu.cn).

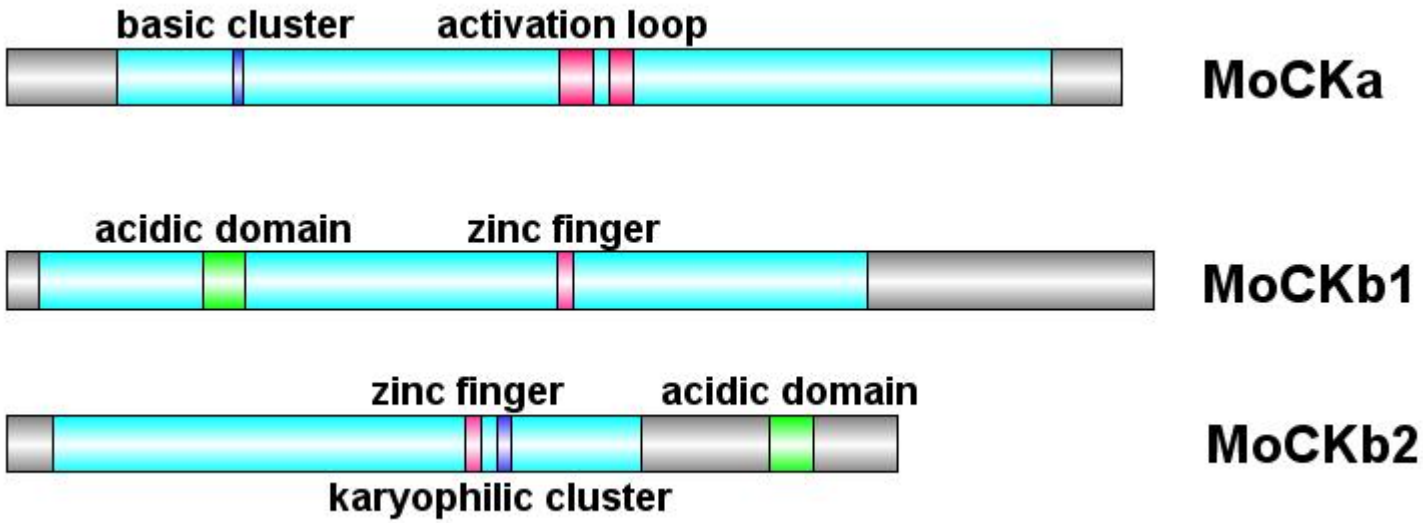

Figure 1. Domain structure of the identified CK2 proteins.
MoCKa sequence (341 aa) was obtained from NCBI and the 35-320 region contains the protein kinase domain (https://www.ncbi.nlm.nih.gov/nuccore/XM_003716137.1) is labelled light blue, 70-73 is the basic cluster labelled dark blue and functions as a nuclear localization signal (NLS), 170-180 and 185-192 are activation loops (A-loop) labelled red.
MoCKb1 sequence (351 aa) was obtained from NCBI and the 11-264 region contains the Casein kinase II regulatory domain (https://www.ncbi.nlm.nih.gov/protein/XP_003718622.1) labelled light blue, 61-74 is the acidic domain labelled green, 169-174 is the zinc finger domain labelled pink.
MoCKb2 sequence (273 aa) was obtained from NCBI and the 15-195 region is the Casein kinase II regulatory subunit domain (https://www.ncbi.nlm.nih.gov/protein/XP_003710544.1) labelled light blue, 141-146 is a zinc finger labelled pink, 151-155 is a karyophilic cluster labelled dark blue that functions as a NLS, 234-247 is an acidic domain labelled green. The illustration was made using the DOG 2.0 Visualization of Protein Domain Structures http://dog.biocuckoo.org/.

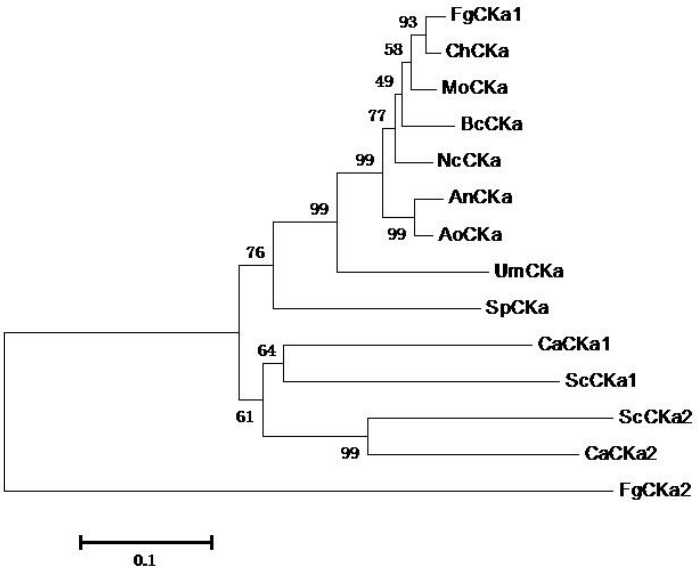

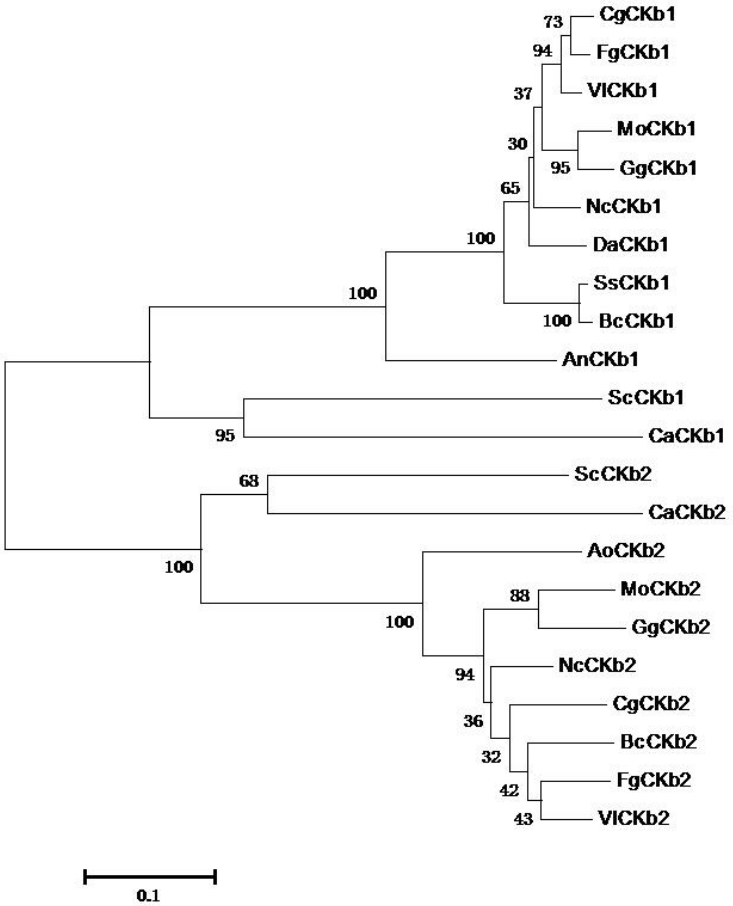

Figure 1 Supplement 1 (**a**) Phylogenetic analysis of CKa amino acid sequences from a range of organisms. A neighbor-joining tree was constructed from amino acid sequences of a range of CKa-encoding genes from diverse fungi. Tree topology was tested by 1000 bootstrap resampling of the data. Full species names and access codes for the annotated genes are given in Figure 1 Supplement 2 legend. **(b)** Phylogenetic analysis of CKb amino acid sequences from a range of organisms. A neighbor-joining tree was constructed from amino acid sequences of a range of CKb-encoding genes from diverse fungi. Tree topology was tested by 1000 bootstrap resampling of the data. Full species names and access codes for the annotated genes are given in Figure 1 Supplement 3 and Figure 1 Supplement 4 legends.

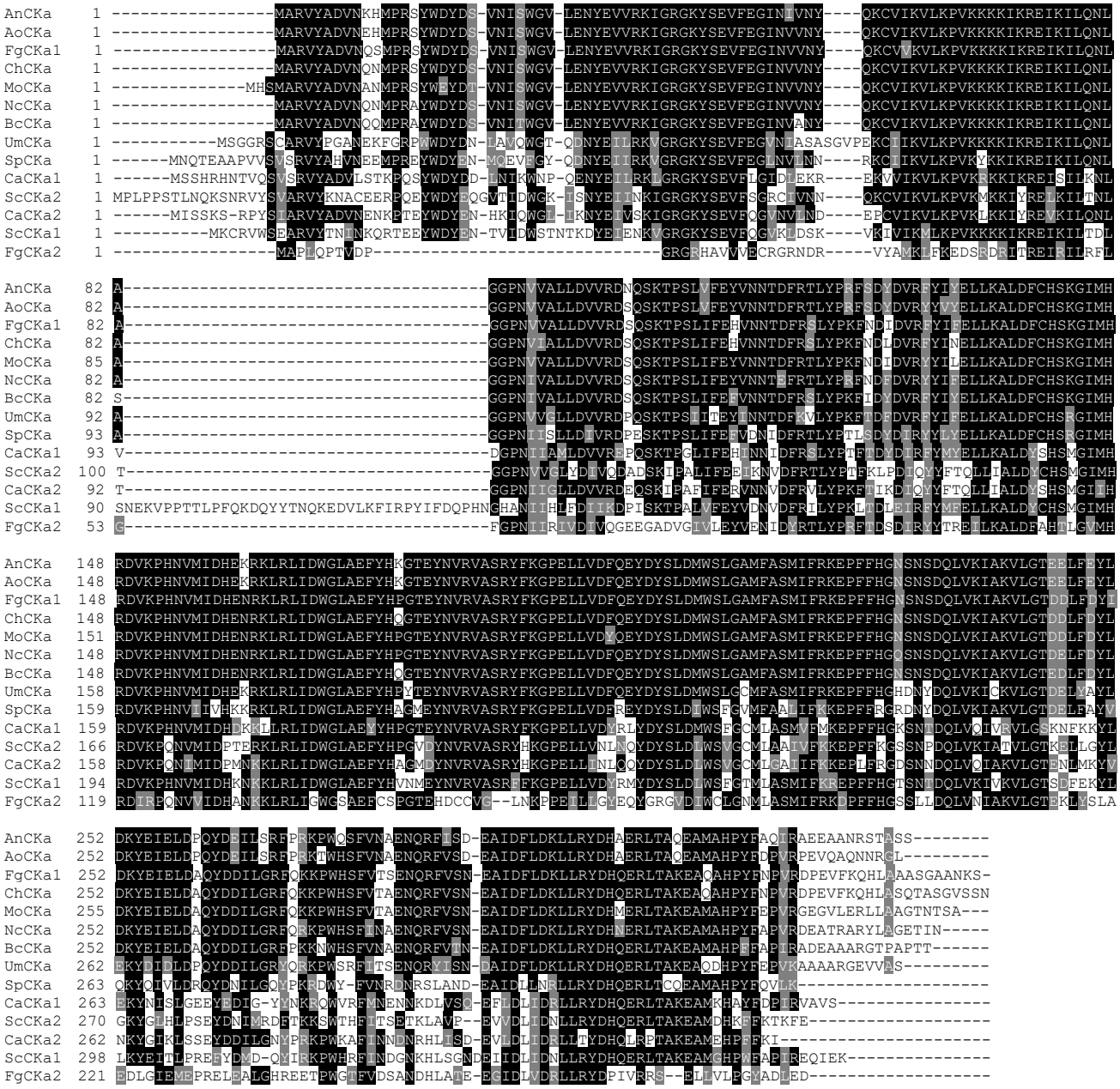

Figure 1 Supplement 2. Alignment of predicted amino acid sequences of CKa from different fungi. Sequence for the CKa in *M. oryzae* and other fungi were aligned using ClustalW and shaded by Boxshade 3.2. Identical amino acids are highlighted on a black background and similar amino acids on a light grey background. The *M. oryzae* amino acid sequence is aligned with the sequences of the putative homologs:

AnCKa (*Aspergillus nidulans*, EAA64615.1),
AoCKa (*Aspergillus oryzae*, KDE76853.1),
FgCKa1 (*Fusarium graminearum*, EYB33507.1),
FgCKa2 (*F. graminearum*, EYB32538.1),
ChCKa (*Colletotrichum higginsianum*, CCF36406.1),
MoCKa (*M. oryzae,* EHA49866.1),
NcCKa (*N. crassa*, EAA35747.3),
BcCKa (*Botrytis cinerea*, EMR85876.1),
UmCKa (*Ustilago maydis*, XP_011387122.1),
SSpCKa (*Schizosaccharomyces pombe*, CAA52331.1),
CaCKa1 (*Candida albicans*, KGU14189.1),
CaCKa2 (*C. albicans*, KGU00855.1),
ScCKa1 (*S. cerevisiae*, EDN61459.1),
ScCKa2 (*S. cerevisiae*, EDN63928.1).

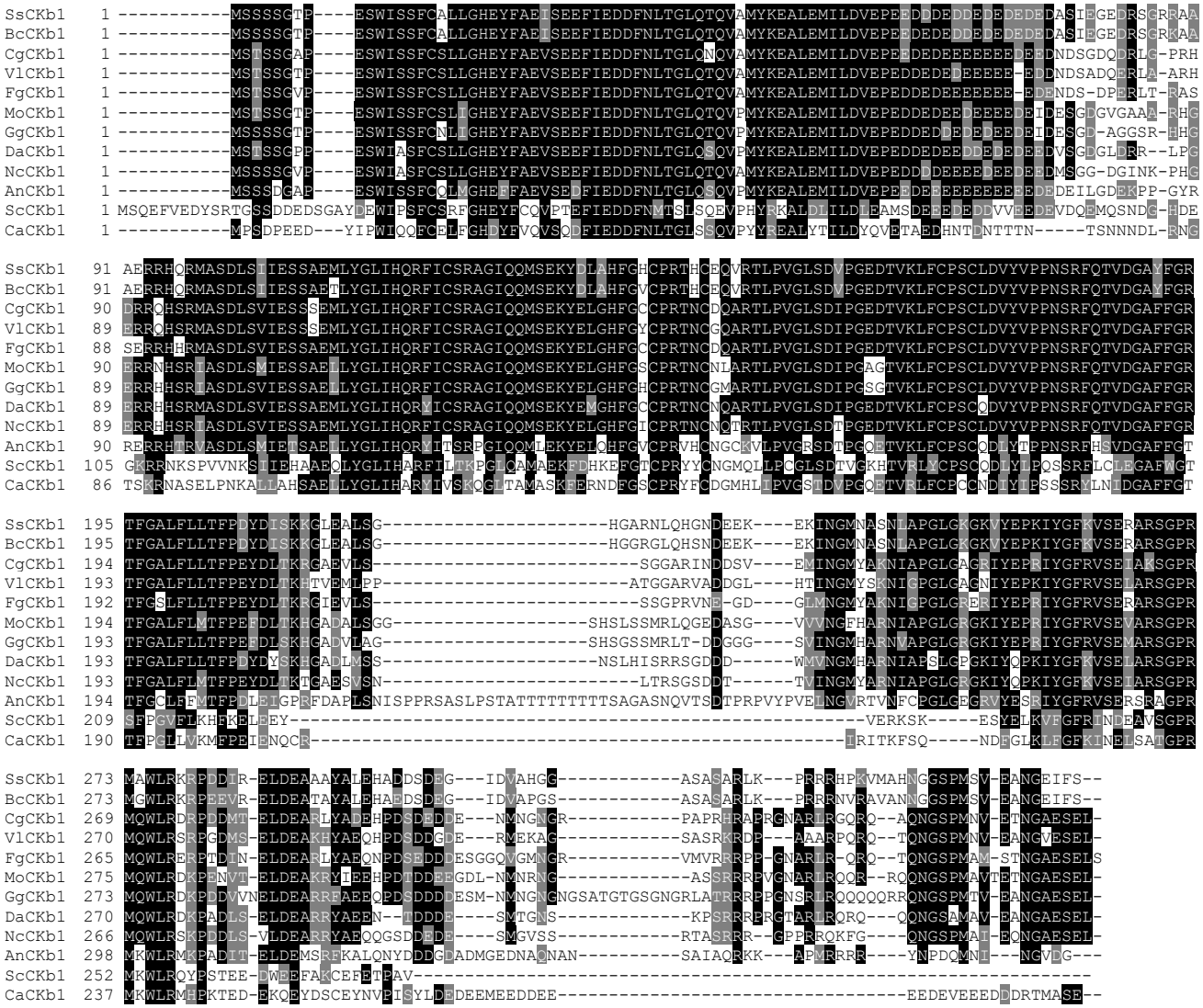

Figure 1 Supplement 3. Alignment of predicted amino acid sequences of CKb1 from different fungi. Sequence for the CKb1 in *M. oryzae* and other fungi were aligned using ClustalW and shaded by Boxshade 3.2. Identical amino acids are highlighted on a black background and similar amino acids on a light grey background. The *M. oryzae* amino acid sequence is aligned with the sequences of the putative homologs:

MoCKb1 (*M. oryzae*, XP_003718622.1),
GgCKb1 (*Gaeumannomyces graminis*, XP_009229023.1)
CgCKb1 (*Colletotrichum graminicola*, XP_008099475.1),
NcCKb1 (*N. crassa*, XP_960447.1),
FgCKb1 (*F. graminearum*, XP_011320142.1),
SsCKb1 (*Sclerotinia sclerotiorum*, XP_001592667.1),
BcCKb1 (*B. cinerea*, XP_001546938.1),
DaCKb1 (*Diaporthe ampelina*, KKY35702.1),
VlCKb1 (*Verticillium longisporum*, CRK29524.1),
AnCKb1 (*A. nidulans*, CBF77758.1),
ScCKb1 (*S. cerevisiae,* NP_011496.3),
CaCKb1 (*C. albicans*, KHC46950.1).

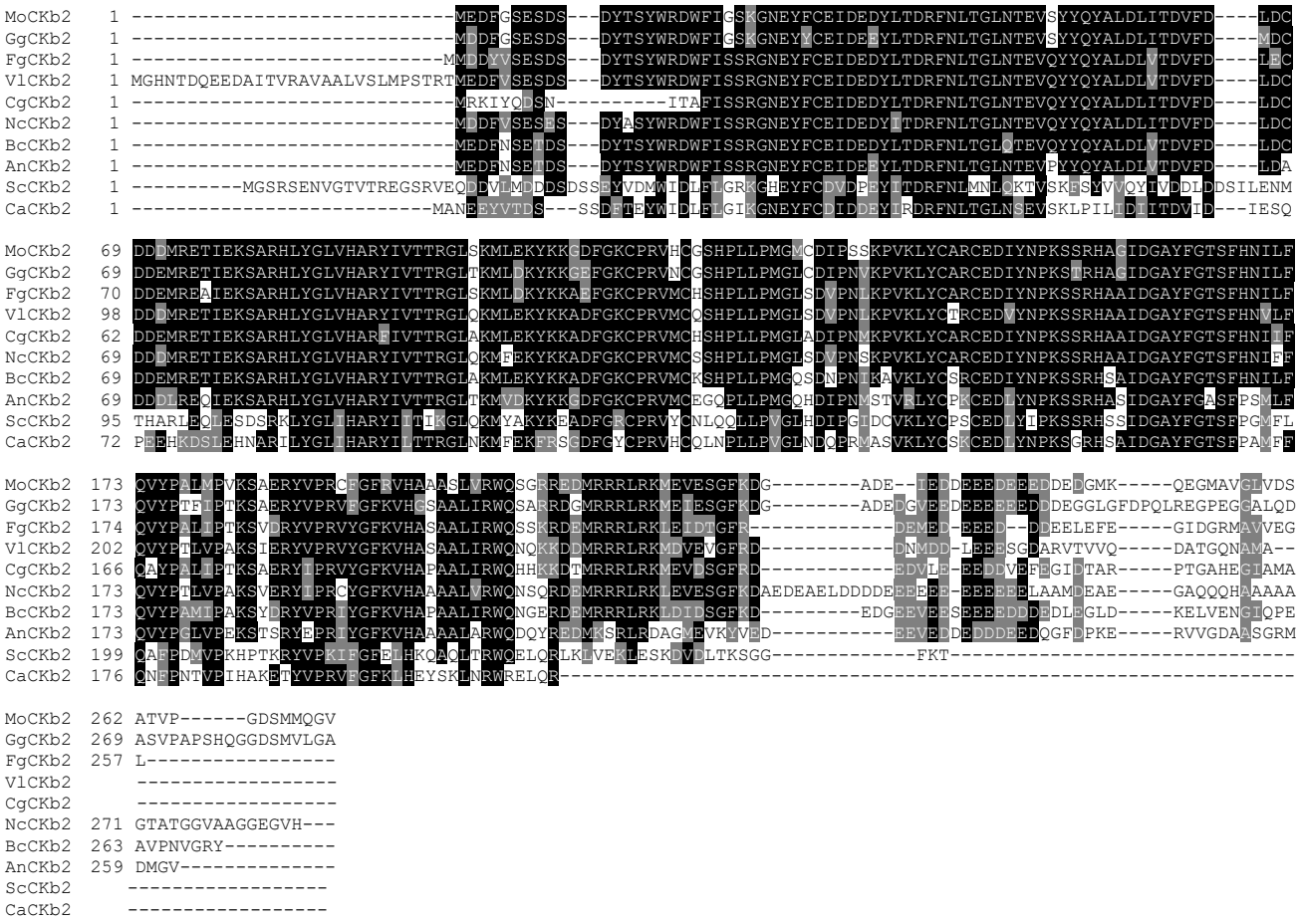

Figure 1 Supplement 4. Alignment of predicted amino acid sequences of CKb2 from different fungi. Sequence for the CKb2 in *M. oryzae* and other fungi were aligned using ClustalW and shaded by Boxshade 3.2. Identical amino acids are highlighted on a black background and similar amino acids on a light grey background. The *M. oryzae* amino acid sequence is aligned with the sequences of the putative homologs:

MoCKb2 (*M. oryzae*, XP_003710544.1),
GgCKb2 (*G. graminis*, XP_009217338.1),
FgCKb2 (*F. graminearum*, EYB21652.1),
VlCKb2 (*V. longisporum*, CRK18911.1),
CgCKb2 (*C. graminicola*, XP_008092732.1),
NcCKb2 (*N. crassa*, XP_001728406.1),
BcCKb2 (*B. cinerea*, XP_001558441.1),
AnCKb2 (*A. nidulans*, XP_001825358.2),
ScCKb2 (*S. cerevisiae*, AAT93000.1),
CaCKb2 (*C. albicans*, EEQ46313.1).

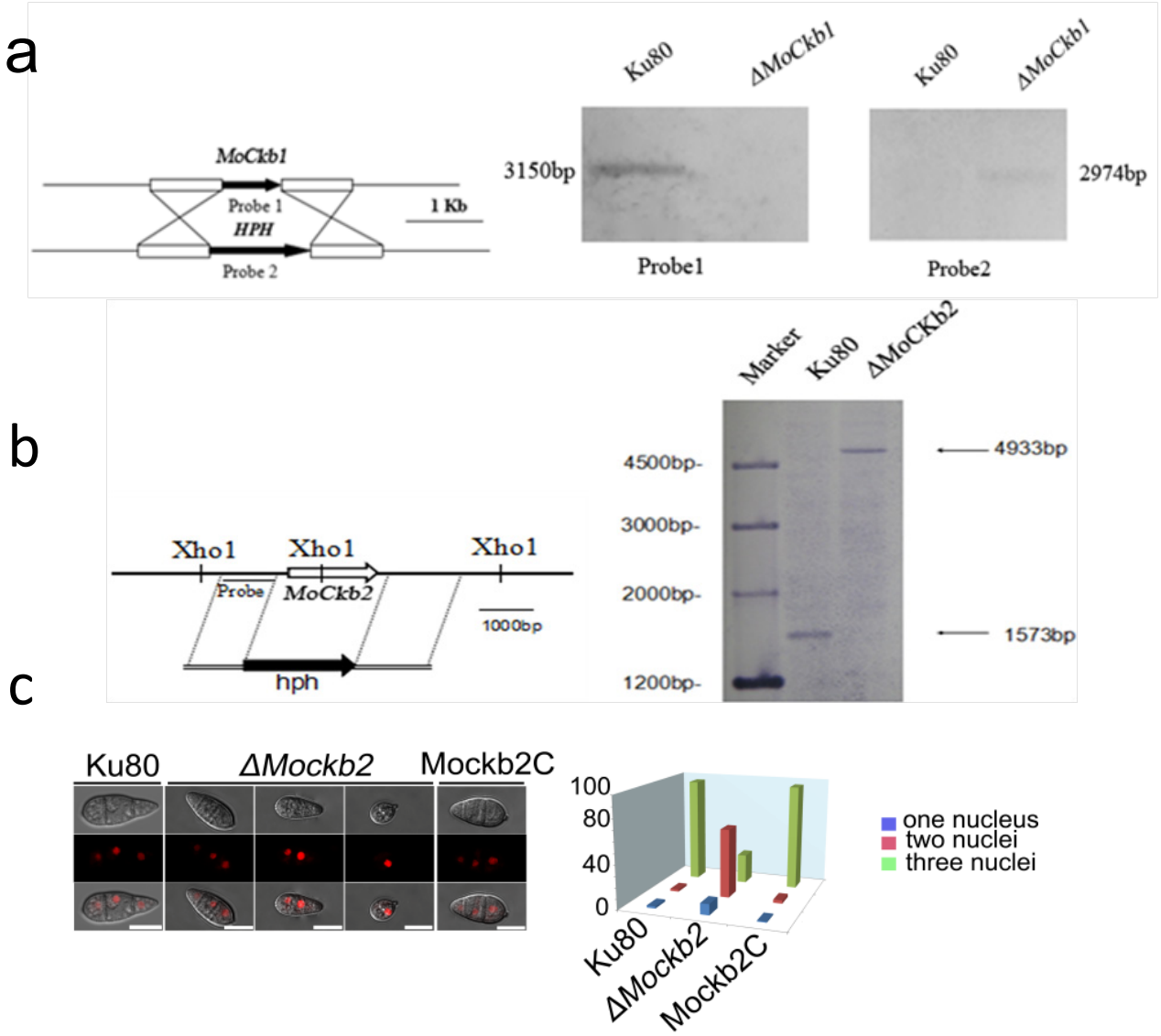

Figure 2. Knockout of the MoCKbs and the effect of this on conidia morphology and MoCKa gene expression (**a**) *ΔMoCkb1* mutant was verified by Southern blot analysis. The genomic DNA extracted from the strains Ku80 and the mutant *ΔMoCkb1* was digested with *Nde1* and tested by Southern blot. The different probes ORF and hph were amplified from the genomic DNA of the wild type Ku80 and the plasmid pCX62 respectively.
(**b**) *ΔMoCkb2* mutant was verified by Southern blot analysis. The genomic DNA extracted from the strains *Ku80* and the mutant *ΔMoCkb2* was digested with *Xho1* and tested by Southern blot. The probe was amplified from the genomic DNA of the background strain Ku80.
(**c**) The conidial morphology of the *ΔMockb2* deletion was detected. The red fluorescence show the nuclear number in the conidia. The red fluorescence was due to the nuclear protein histone linker (MGG_12797) fused with mCherry used as nuclear marker. All bars = 10 um. The percentage of conidia with different nuclear number in the conidia produced by the background strain Ku80, the *ΔMockb2* deletion mutant and in the complementation strain MoCKb2C.

Figure 3. Control that GFP-MoCKa, GFP-MoCKb1 and GFP-MoCKb2 are as pathogenic as the background Ku80. CK is untreated control.

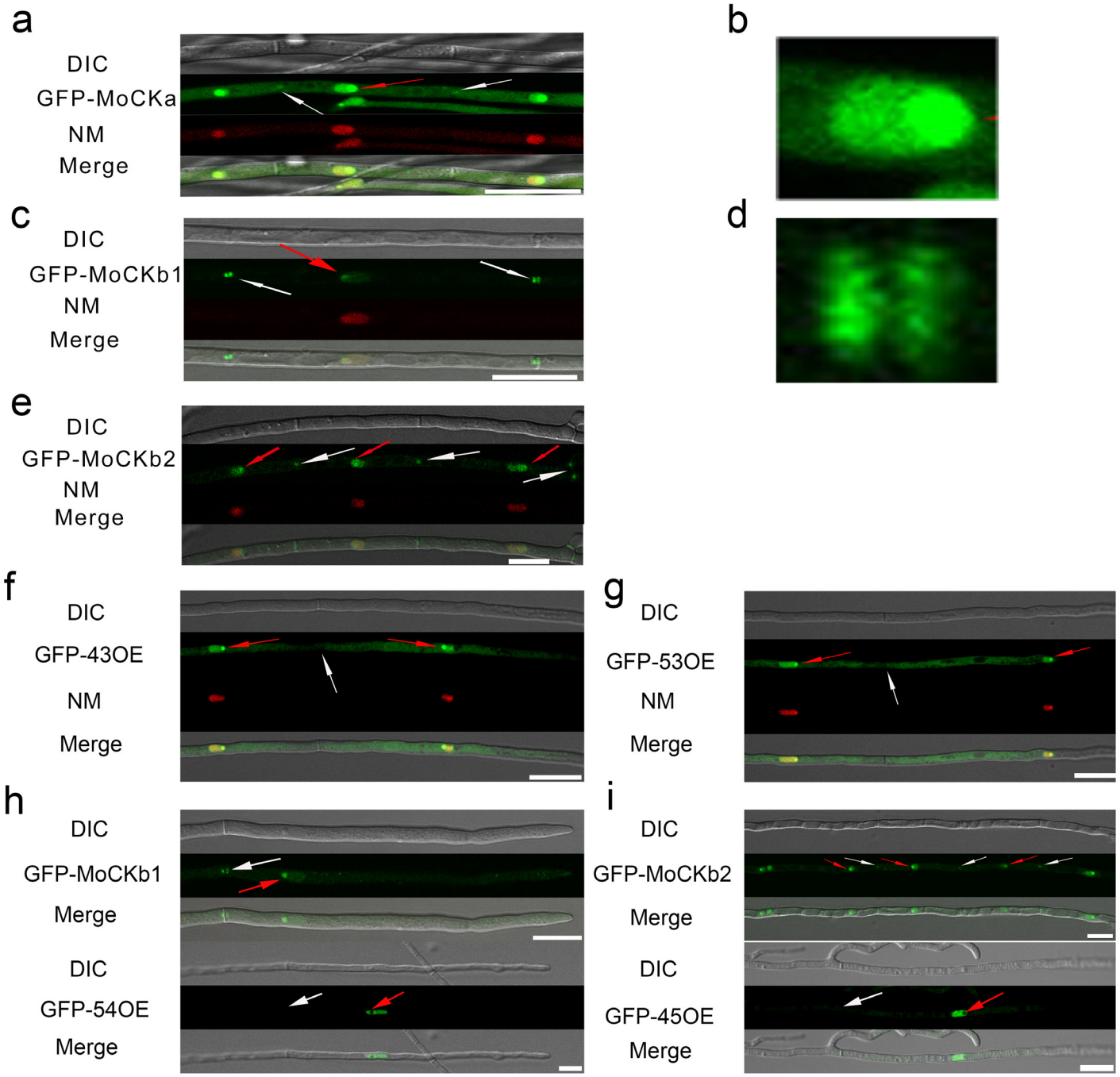

Figure 4. Intracellular localization of the three CK2 holoenzyme components showing that all three proteins are needed for normal localization. a-e, Localization of the three MoCK2 subunits in the background strain Ku80. The background strain Ku80 was transformed through gene replacements using plasmids containing GFP-MoCKa, GFP-MoCKb1 and GFP-MoCKb2. All three GFP constructs localize preferentially to nucleoli and to septal pores between cells. **b**, Enlargement of the nuclear localization of GFP-MoCKa (marked with red arrow in **a**). **d**, Enlargement of the septal localization of GFP-MoCKb1 (left septa marked with white arrow in **c**) **f** and **g**, Localization of over expressed GFP-MoCKa in *ΔMockb1* (43OE-GFP) or in *ΔMockb2* (53OE-GFP) does not rescue normal localization to septal pores. **h** and **i**, (below) Neither overexpression of MoCKb1 in *ΔMockb2* (54OE-GFP) nor overexpression of MoCKb2 in *ΔMockb1* (45OE-GFP) rescued normal localization (GFP-MoCKb1 and GFP-MoCKb2) (above) to nucleoli or septal pores. Histone linker (MGG_12797) was fused with the mCherry and used as nuclear localization marker (NM). All bars=10mm.

Figure 4 Supplement 1.
GFP-MoCKa localization in conidia.

Magnaporthe oryzae conidia.

GFP-MoCKa localizes to nuclei (red arrows) and to septal pores (white arrows). White bar is 10 μm.

a

Expression of	Control	Test	Test/control	SE (N=9)	P=same or higher than control
MoCKa	Ku80	*ΔMoCKb1*	0.38	0.01	2.07E-11
MoCKa	Ku80	*ΔMoCKb2*	0.54	0.05	5.12E-06

b

Expression of	Control	Test	Test/control	SE (N=9)	P=same or lower than control
MoCKa	ΔMoCKb1	43OE	25.11	1.32	4.23E-08
MoCKa	ΔMoCKb2	53OE	14.60	1.45	6.85E-06

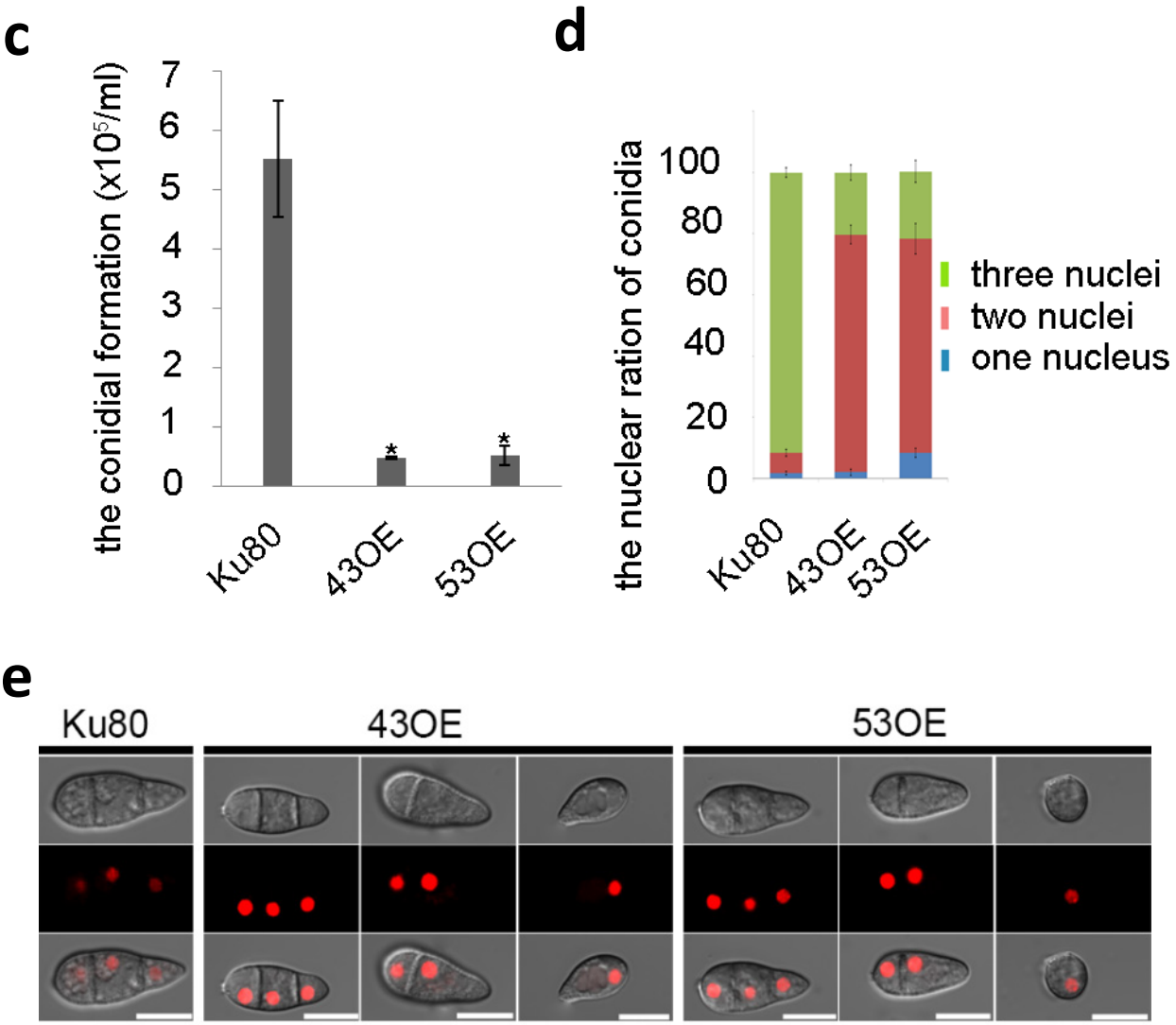

Figure 5. Overexpression of MoCKa in the MoCKb deletion mutants and the effect of this on conidia morphology. (**a**) MoCKa expression in the *ΔMockb1* and *ΔMockb2* deletion relative to the MoCKa expression in the control Ku80 showing that expression of the two CKb were both reduced in the deletion mutants (**b**) The relative expression of MoCKa in the 43OE and 53OE in relation to their respective control backgrounds *ΔMoCKb1* and *ΔMoCKb2*. (**c**) The conidial forming ability of the 43OE and 53OE transformants compared to the background strain Ku80. (**d**) The percentage of conidia with different numbers of nuclei produced by the background strain Ku80 and the 43OE and 53OE strains. (**e**) The conidia morphology of 43OE and 53OE transformants. The red fluorescence was due to the nuclear protein histone linker (MGG_12797) fused with the mCherry. All bars = 10 um.

Figure 5 Supplement 1. The expression the different overexpressed components of the MoCK2 holoenzyme in the Ku80 background and the deletion mutant background in relation to the expression in respective background. The experiments were repeated three times with triple replications.

Expression of	Control	Test	Test/control	SE (N=9)	P=same or lower than control
MoCKa	Ku80	GFP-MoCKa	15.38	0.87	8.80E-08
MoCKb1	Ku80	GFP-MoCKb1	9.51	0.70	1.01E-06
MoCKb2	Ku80	GFP-MoCKb2	14.64	0.85	1.14E-07
MoCKb2	*ΔMoCKb1*	45OE	12.63	1.35	1.26E-05
MoCKb1	*ΔMoCKb2*	54OE	45.47	2.52	5.43E-08

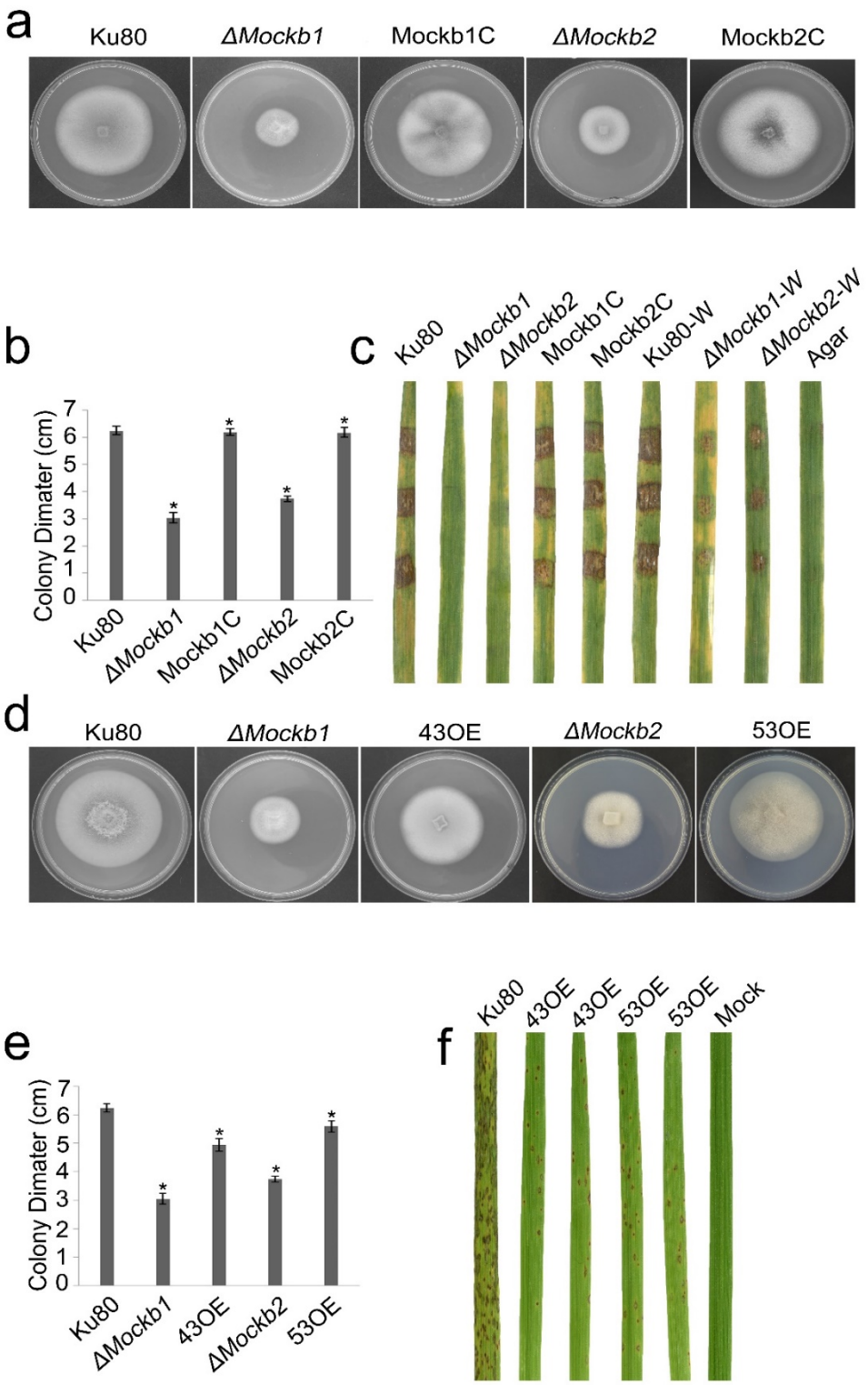

Figure 6. Intact CK2 holoenzyme is needed for normal growth, infection, pathogenicity. a, Colonial morphology and **b,** vegetative growth of *ΔMockb1* and *ΔMockb2* deletion mutants and their respective complementation strains was observed on SYM agar plates incubated in the dark for 10 days at 25°C, and then photographed. **c,** Pathogenicity analysis of *ΔMockb1* and *ΔMockb2* on rice. Disease symptoms on rice leaves of 2-week-old seedlings inoculated using mycelial plugs since mutants produced no or very few conidia. Typical leaves were photographed 6 days after inoculation. The Mockb1C and Mockb2C were complementary strains. Treatments ending with a W indicate that the leaf surface was wounded before the plug was applied. The rice cultivar was CO-39. **d,** Colonial morphology and **e,** vegetative growth of *ΔMockb1*, *ΔMockb2*, and overexpressed CKa-GFP in the *ΔMockb1* (43OE) and in *ΔMockb2* (53OE) transformants were observed on SYM medium agar plates incubated in the dark for 10 days at 25°C, and then photographed. **f,** Pathogenicity analysis of overexpressed CKa-GFP in the *ΔMockb1* (43OE) and in *ΔMockb2* (53OE). Disease symptoms on rice leaves of 2-week-old seedlings inoculated with conidia suspension since CKa overexpressed strains produced just enough conidia to use for the assay. The concentration of conidia in the suspension was about 1×10^5/ml. Typical leaves were photographed 6 days after inoculation. The rice cultivar was CO-39. Error bars shows SE and a star indicate a $P<0.05$ for control is same or larger than for the mutants.

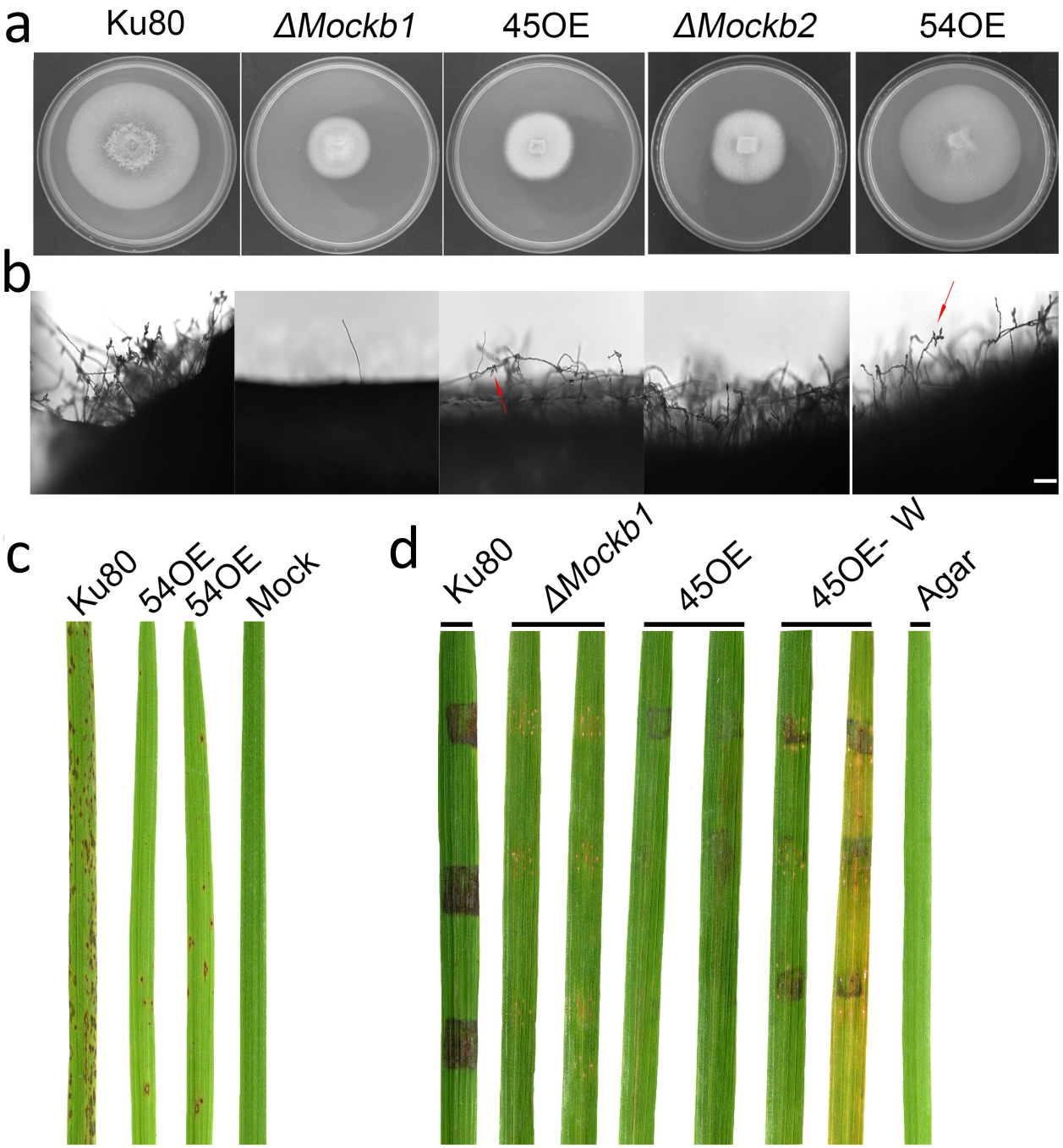

Figure 6 Supplement 1. Phenotypic effects in the respective MoCKb deletion mutants of overexpression the other MoCKb component. (**a** and **c**) Colonial morphology and vegetative growth of *ΔMockb1*, 45OE transformants, *ΔMockb2* and 54OE transformants was observed on SYM medium agar plates grown in the dark for 10 days at 25 °C and then photographed.
(**b**) Development of conidia on conidiophores. Light microscopic observation was performed on strains grown on the rice bran medium for 10 days. The red arrows indicate some conidia are produced by the 45OE and 54OE transformants. Bar=50um.
(**c**) Pathogenic analysis of 54OE transformants on rice was shown above. Disease symptoms on rice leaves of 2-week-old seedlings were also inoculated by conidia suspension. The concentration of conidia suspension for inoculation was about $1x10^5$/ml.
(**d**) Pathogenic analysis of *ΔMockb1* and 45OE transformants on rice. Disease symptoms on rice leaves of 3-week-old seedlings were also inoculated using mycelial plugs. The 45OE-W indicates that the rice leaves were wounded. Typical leaves were photographed 6 days after inoculation. The rice strain was CO-39.

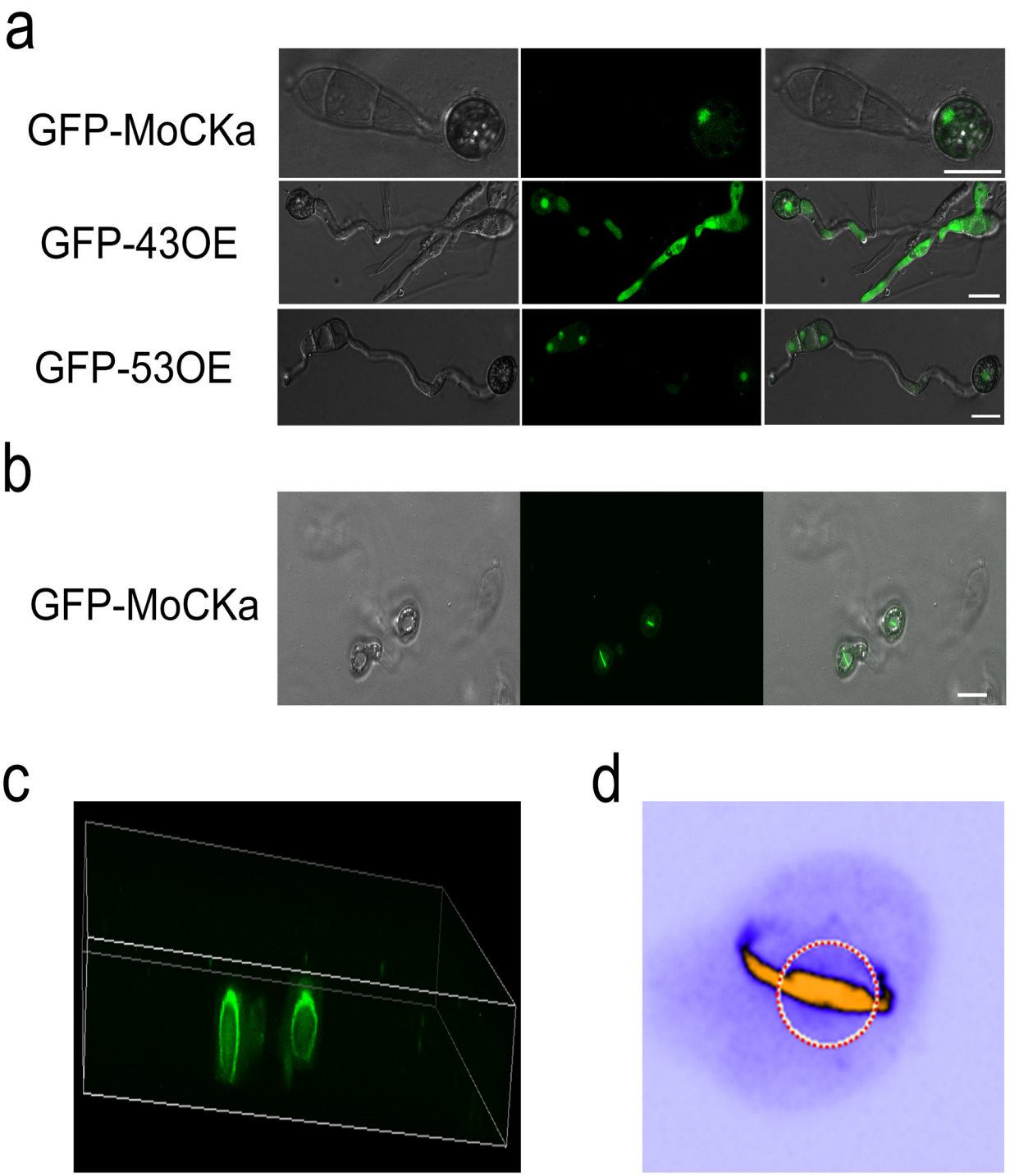

Figure 7. Localization of the GFP-MoCKa subunit in appressoria of the background strain Ku80 the and in the two MoCKb deletion strains (43OE-GFP and 53OE-GFP) (compare Fig. 1a, f, g). **a,** Localization of GFP-MoCKa in all three strains show localization to nuclei**. b,** In the background strain Ku80 that form appressoria from conidia a bright line of GFP-MoCKa can be seen across the appressorium penetration pores. **c.** Through 3d scanning and then rotating the 3d reconstruction image (Link to Movie 1) we found that the streak across the penetration pores is a ring of GFP-MoCKa perpendicular to the penetration pore opening not present in the deletion strains (Link to Movie 2 and 3). **d,** False colour lookup table 3d reconstruction image of the right ring structure in **c** enlarged and rotated back and seen from the same angle as in **b** with the penetration pore opening indicated by a red-white circle seen from the "plant" side (Link to Movie 4 and 5 for left and right ring in false colours). The false colour was used so that the week fluorescence in the cytoplasm could be used to show the whole cytoplasm volume. The image was made using the analytical image analysis freeware ImageJ (https://imagej.nih.gov/ij/index.html) and the ICA lookup table in ImageJ was used for false colouring. **e**, Measurements of the sizes of the GFP-MoCKa rings in seen in **c.** All bars=10 mm.

Figure 7 Supplement 1.
GFP-MoCKa localization in appressoria.

Magnaporthe oryzae appressoria. Image in the 3d stack (left appressorium in Fig. 3b,d) that shows the septal pore accumulation. Image deliberately ”overexposed” to be able to show nuclear and septal localization.

GFP-MoCKa localizes to nuclei (red arrow) surrounded by the large ring structure in cross-section (blue arrows) and to the septal pore towards the germtube (white arrow). White bar is 10 μm.

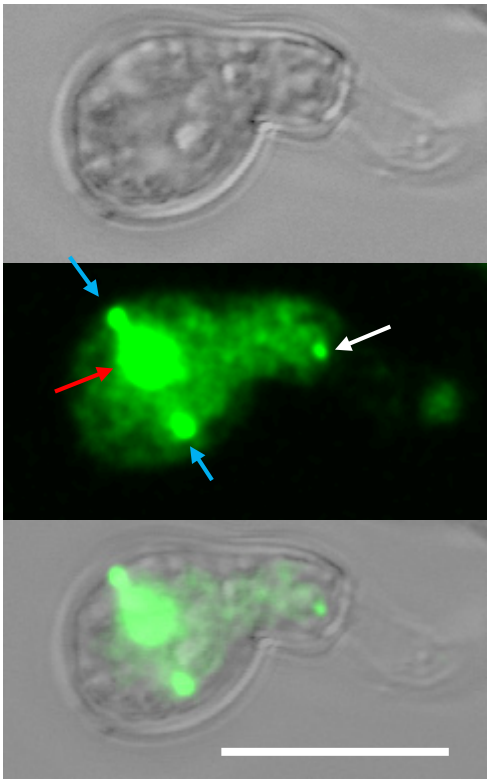

Figure 7 Supplement 2.

MoCK2 Rings	Right	Left
Measurements from images	um	um
Outer diameter	5.3	5.5
Max thickness at penetration pore	1.4	1.2
Thickness on sides and away from pore	0.7	0.7
Thickness seen from side	0.7	0.7

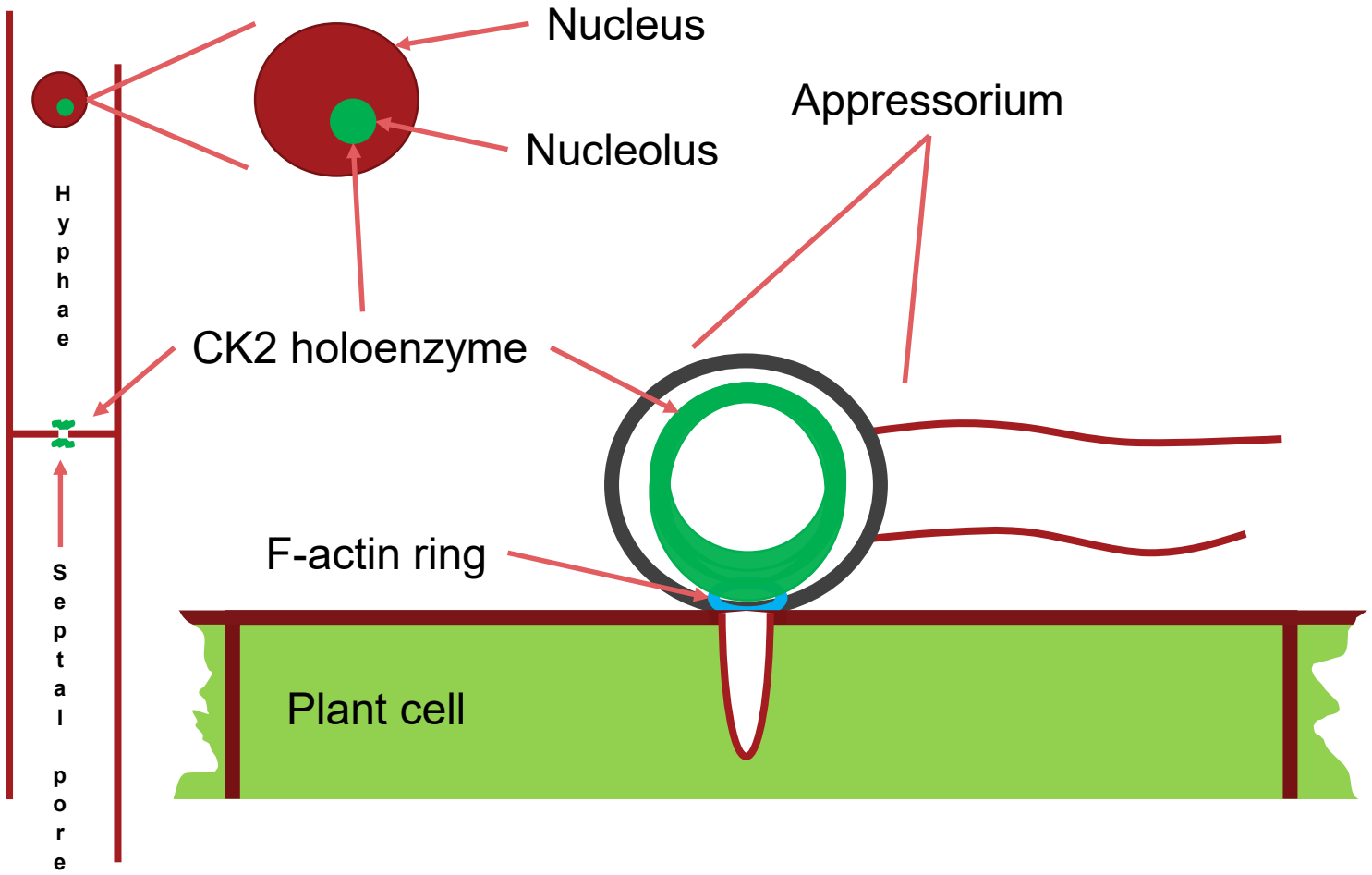

Figure 8. Schematic drawing of the main localizations of the CK2 holoenzyme. It localizes to the nucleolus, to septal pores between cells and forms a large ring structure perpendicular to the F-actin ring surrounding the appressorium penetration pore. Appressorium and hyphae drawn approximately to their relative sizes.

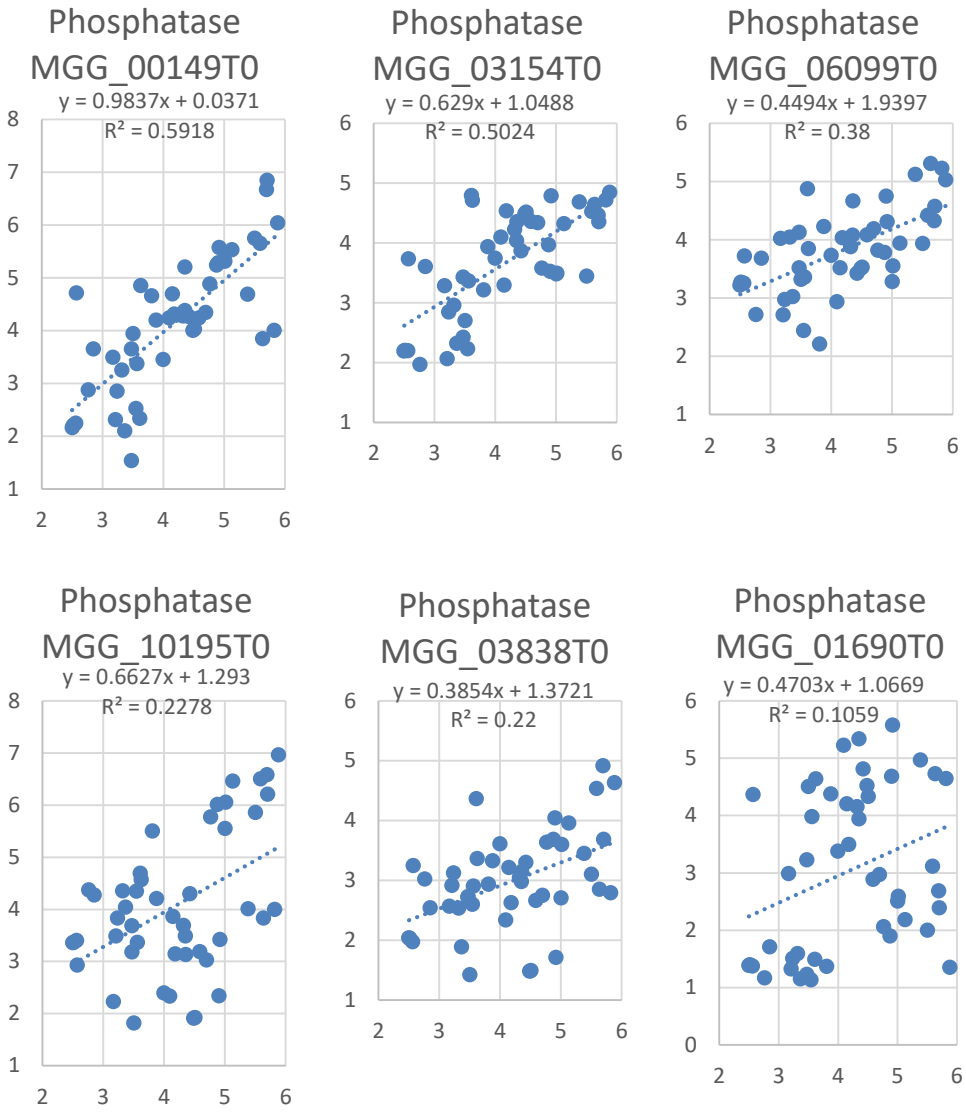

Figure 9. Plots of 6 putative serine/threonine protein phosphatase expression (y-axis) vs MoCKa expression (x-axis) in a range of transcriptome datasets from different experiments (Note: Log2 scale on axes and grids are represented with fixed "aspect ratio" to highlight the different slopes of the correlations). MGG_01690 is not in the pulldown while the other five are and used to illustrate that not all S/T phosphatases are well correlated with CKa. The P values for the Null hypothesis of no correlation with CKa are: MGG_00149 P=2.7E-10, MGG_03154 P=2.5E-8, MGG_06099 P=4.0E-6, MGG_10195 P=6.9E-4, MGG_03838 P=8.8E-4, MGG_01690 P=2.6E-2
Transcriptomic data was downloaded from public websites so as to be able to test the relationship under many different growth conditions in many experiments.

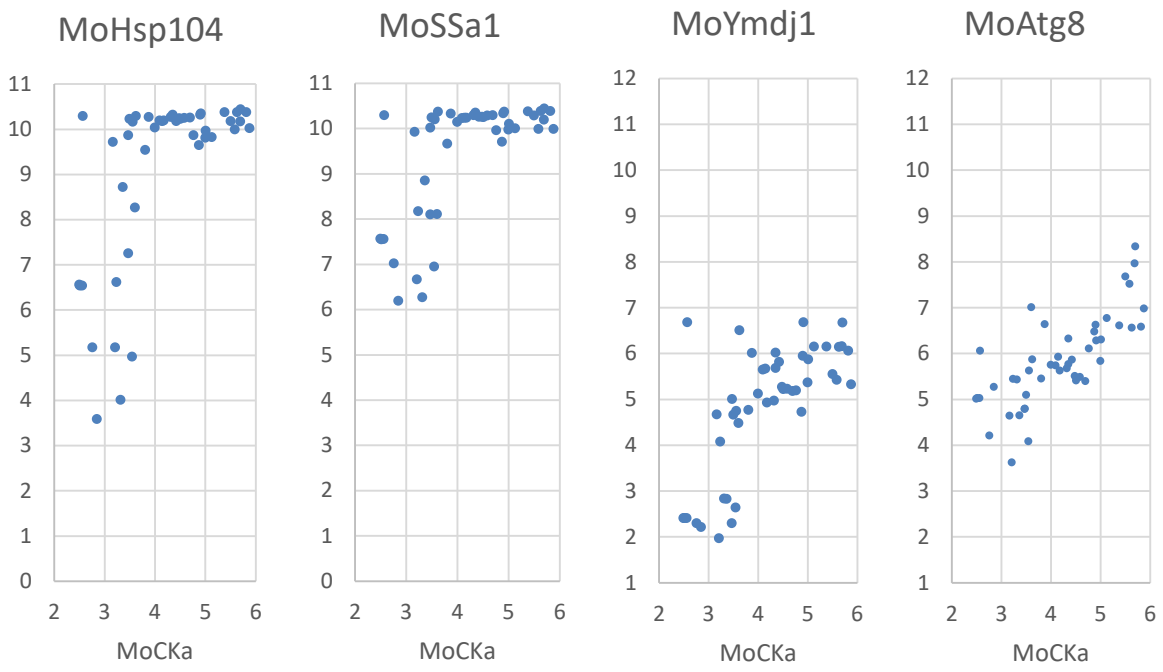

Figure 10 Plot of expression involved in protein quality control vs MoCKa expression in a range of transcriptomes from different experiments (Note: Log2 scale on axes and grids are represented with fixed "aspect ratio“ to highlight the slope of the correlation). P value for the Null hypothesis that there is no correlation = 9.9E-10. Transcriptomic data was downloaded from public websites so as to be able to test the relationship under many different growth conditions in many experiments.
Hsp104, SSa1 and Ymdj1 has in yeast been shown to cooperatively help aggregate proteins to be able to refold. The key protein with its main function in this process appear to be Hsp104 (Glover and Lindquist, 1998).

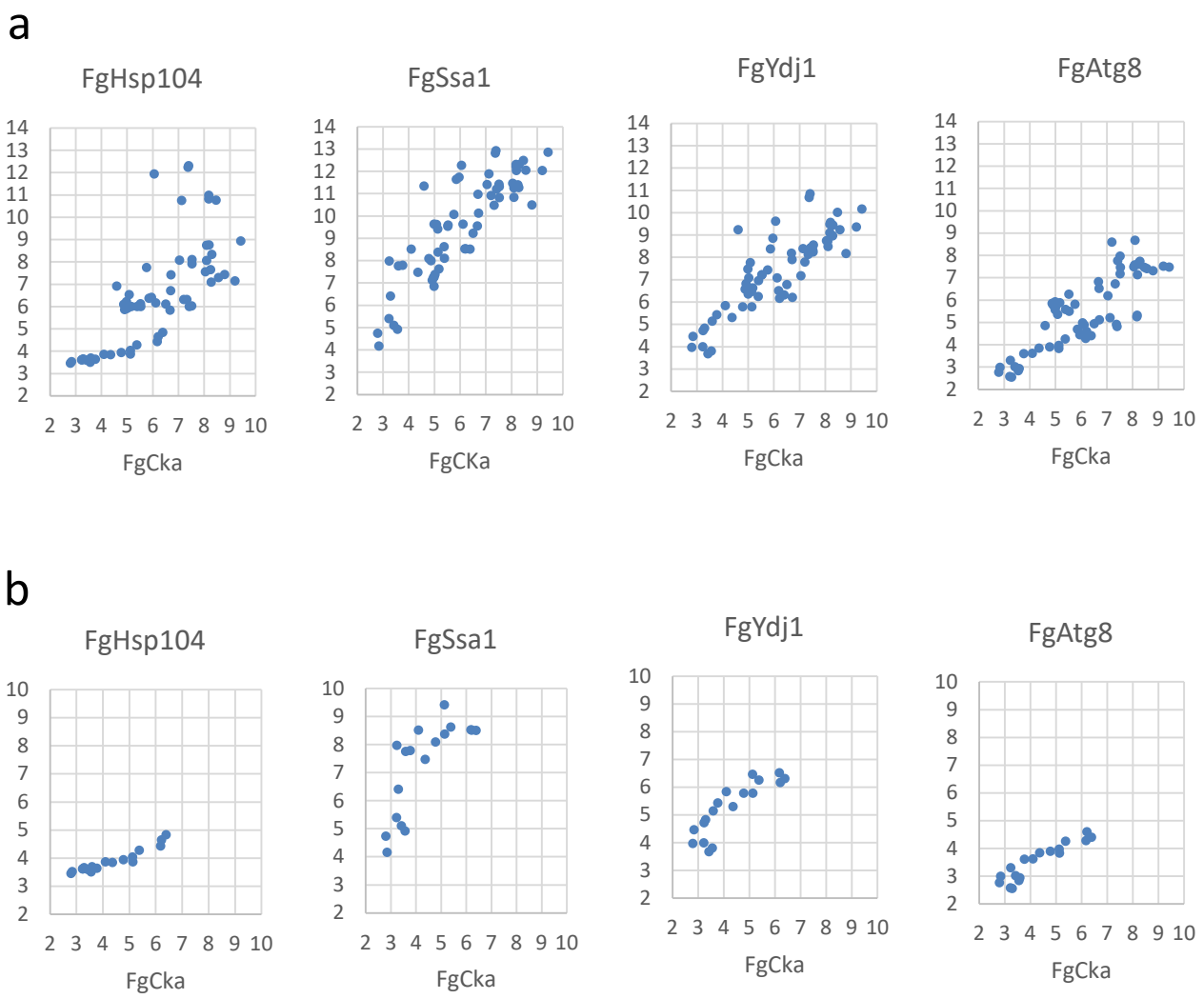

Figure 10 Supplement 1. Plot of expression involved in protein quality control vs FgCKa expression in a range of transcriptomes from different experiments (Note: Log2 scale on axes and grids are represented with fixed "aspect ratio" to highlight the slope of the correlation). a. data from all experiments. b data from a time course infection experiment (see Fig 10 supplement 2 for details on the time course of expression)

Transcriptomic data was downloaded from public websites so as to be able to test the relationship under many different growth conditions in many experiments.

Hsp104, SSa1 and Ymdj1 has in yeast been shown to cooperatively help aggregate proteins to be able to refold. The key protein with its main function in this process appear to be Hsp104 (Glover and Lindquist, 1998) .

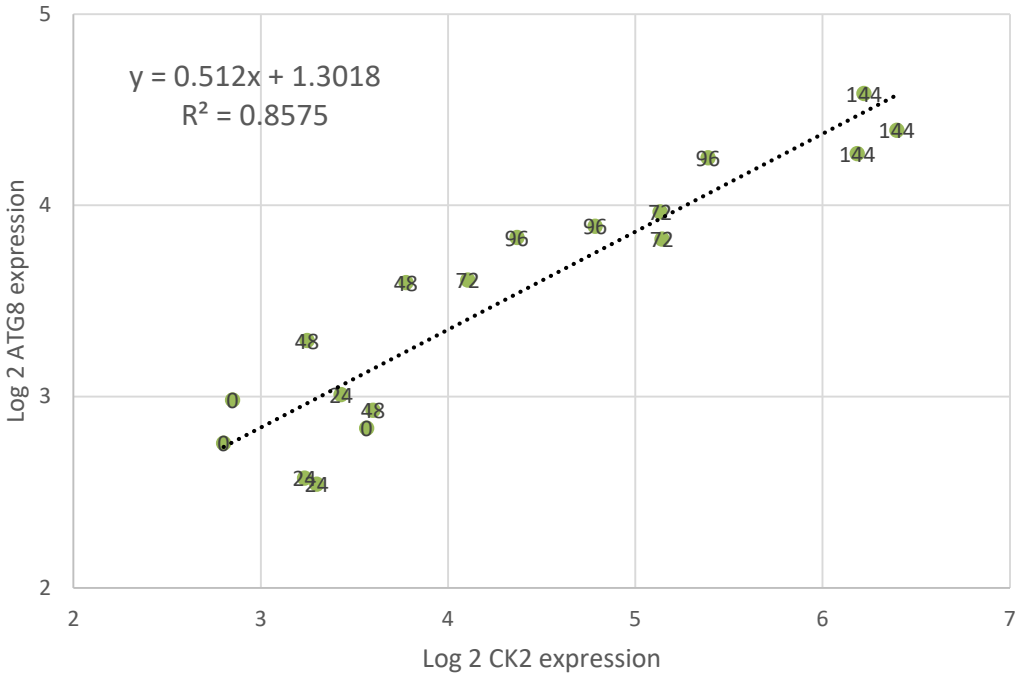

Figure 10 Supplement 2. Plot of FgAtg8 (autophagy) expression vs FgCKa expression in a times series infection experiment with 3 replicates where numbers in the plot indicate hours post infection (hpi). (Note: Log2 scale on axes and grids are represented with fixed "aspect ratio“ to highlight the slope of the correlation). P value for the Null hypothesis that there is no correlation = 3.6E-08 . Transcriptomic data was downloaded from public websites so as to be able to test the relationship under many different growth conditions in many experiments.

Table 1 Background and mutant strains of *M. oryzae* used in this study

Strains	Genotype description	Reference
Ku80	*ku80* deletion mutant of Guy11 (Background strain in this study)	35
ΔMockb1	*Mockb1* deletion mutant of *Ku80*	This study
ΔMockb2	*Mockb2* deletion mutant of *Ku80*	This study
Mockb1C	*ΔMockb1* transformed with the wild-type MoCKb1 protein	This study
Mockb2C	*ΔMockb2* transformed with the wild-type MoCKb2 protein	This study
53OE	*ΔMockb2* transformed with the over-expressed GFP-MoCKa fusion protein	This study
43OE	*ΔMockb1* transformed with the over-expressed GFP-MoCKa fusion protein	This study
54OE	*ΔMockb2* transformed with the over-expressed GFP-MoCKb1 fusion protein	This study
45OE	*ΔMockb1* transformed with the over-expressed GFP-MoCKb2 fusion protein	This study
GFP-MoCKa	Ku80 transformed with the over-expressed GFP-MoCKa fusion protein	This study
GFP-MoCKb1	Ku80 transformed with the over-expressed GFP-MoCKb1 fusion protein	This study
GFP-MoCKb2	Ku80 transformed with the over-expressed GFP-MoCKb2 fusion protein	This study

Table 2 Primers used in this study

Primer name	The sequence of primer（5’→ 3’）
3696qRTF	CGTCAACTACCAGAAATGCG
3696qRTR	TGACGGAGTCTTGCTCTGTG
446qRTF	GCAGAGGTGTCGGAGGAAT
446qRTR	CCAAGATCATCTCCAGTGCC
5651qRTF	ACCCGTTGCTGCCGATGG
5651qRTR	TAGACCTGGAAGAGGATGTTGTGG
Tub1RTF	CAACATCCAGACCGCTCTC
Tub1RTR	ACCGACACGCTTGAACAG
446AF	GCCCAACCTTTCATCCTA
446AR	TTGACCTCCACTAGCTCCAGCCAAGCCTACCTCCAGTGCCTCCTT
446BF	GAATAGAGTAGATGCCGACCGCGGGTTCTCGTCCAACTCTAAACTAAC
446BR	GCTGGGTAAACATCTCATT
5651AF	GGGGTACCCCCTCTAAGTGGTCGTGC
5651AR	CCGGAATTCCTTGGATGGAATTGTGCC
5651BF	CGCGGATCCAGGGAGGCGTTATCATTTA
5651BR	TAATCTAGACAGAGCCGAGCTTGTCTA
446comF	GCTCTAGAGCGGAACCAGTAGTTGACGG
446comR	GGGGTACCCATGACAACGCCGGAGGG
5651comF	GCTCTAGAGCCCGACAAGCACAAAAGAT
5651comR	CCCCCGGGGAGCGTTCGTTTAGACCC
3696GFPF	CGGGATCCATGCACAGCATGGCACGC
3696GFPR	CGGAATTCTGTTGAAATTACCAGCGATTC
5651GFPF	CGGGATCCATGGAAGATTTTGGCAGCG
5651GFPR	CCCTCGAGTCAGACACCTTGCATCATG